The Journal of Physiology

Kappa opioids inhibit the GABA/glycine terminals of rostral ventromedial medulla projections in the superficial dorsal horn of the spinal cord

Yo Otsu[1,2] and Karin R. Aubrey[1,2]

[1]*Pain Management Research, Kolling Institute at the Royal North Shore Hospital NSLHD, University of Sydney, St Leonard, New South Wales, Australia*
[2]*Faculty of Medicine and Health - Northern, Sydney Pain Consortium, University of Sydney, Camperdown, New South Wales, Australia*

Handling Editors: Katalin Toth & Samuel Young

The peer review history is available in the Supporting Information section of this article (https://doi.org/10.1113/JP283021#support-information-section).

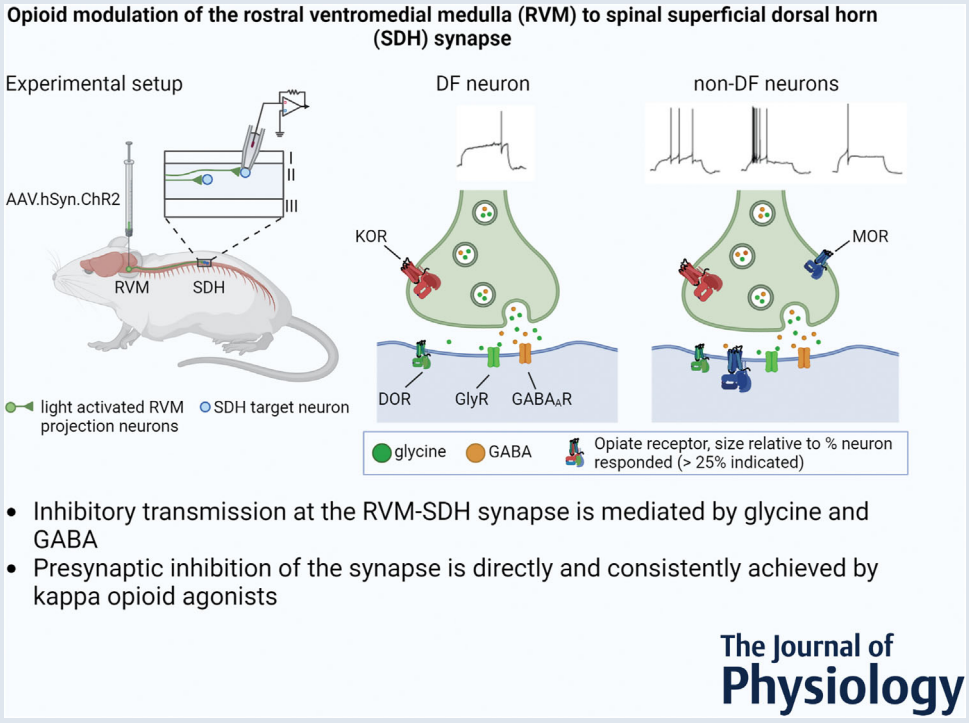

Abstract Descending projections from neurons in the rostral ventromedial medulla (RVM) make synapses within the superficial dorsal horn (SDH) of the spinal cord that are involved in the modulation of nociception, the development of chronic pain and itch, and an important analgesic target for opioids. This projection is primarily inhibitory, but the relative contribution of GABAergic and glycinergic transmission is unknown and there is limited knowledge about the SDH neurons targeted. Additionally, the details of how spinal opioids mediate analgesia remain unclear, and no study has investigated the opioid modulation of this synapse. We address this using *ex vivo* optogenetic stimulation of RVM fibres in conjunction with whole-cell patch-clamp

This article was first published as a preprint. Otsu Y, Aubrey K. 2021. Kappa opioids inhibit the GABA/glycine terminals of rostral ventromedial medulla projections in the superficial dorsal horn of the spinal cord. Authorea. https://doi.org/10.22541/au.163855174.47774331/v1.

© 2022 The Authors. *The Journal of Physiology* published by John Wiley & Sons Ltd on behalf of The Physiological Society.
This is an open access article under the terms of the Creative Commons Attribution-NonCommercial License, which permits use, distribution and reproduction in any medium, provided the original work is properly cited and is not used for commercial purposes.

DOI: 10.1113/JP283021

recordings from the SDH in spinal cord slices. We demonstrate that both GABAergic and glycinergic neurotransmission is employed and show that SDH target neurons have diverse morphological and electrical properties, consistent with both inhibitory and excitatory interneurons. Then, we describe a subtype of SDH neurons that has a glycine-dominant input, indicating that the quality of descending inhibition across cells is not uniform. Finally, we discovered that the kappa-opioid receptor agonist U69593 presynaptically suppressed most RVM-SDH synapses. By contrast, the mu-opioid receptor agonist DAMGO acted both pre- and postsynaptically at a subset of synapses, and the delta-opioid receptor agonist deltorphin II had little effect. These data provide important mechanistic information about a descending control pathway that regulates spinal circuits. This information is necessary to understand how sensory inputs are shaped and develop more reliable and effective alternatives to current opioid analgesics.

(Received 24 February 2022; accepted after revision 22 July 2022; first published online 18 August 2022)
Corresponding author Karin R. Aubrey: Pain Management Research Laboratories, Kolling Institute and University of Sydney, Level 13 Kolling Building (E25K), Royal North Shore Hospital, St Leonards, NSW 2065, Australia. Email: karin.aubrey@sydney.edu.au

Abstract figure legend We combined *ex vivo* optogenetic stimulation of RVM fibres with whole cell electrophysiology of SDH neurons to investigate the final synapse in a key descending pain modulatory pathway. We demonstrate that both glycine and GABA mediate signalling at the RVM-SDH synapse, that the SDH targets of RVM projections have diverse electrical and morphological characteristics, and that presynaptic inhibition is directly and consistently achieved by kappa opioid agonists. Opioid receptors shown are sized relative to the proportion of neurons that responded to its specific agonists (81% and 84% of DF and non-DF neurons responded to kappa opioid receptor agonists, respectively. Responses that occurred in <25% of neurons are not indicated).

Introduction

Incoming noxious signals received by the superficial dorsal horn (SDH) are strongly modified by descending fibres that originate in higher brain regions including the brainstem and the cerebral cortex (Millan, 2002). The brainstem rostral ventromedial medulla (RVM), which includes the raphe magnus and gigantocellular reticular nucleus alpha, projects to the SDH to form the final synapse of a key descending pathway from these higher centres which has an important role in modulating pain transmission at the spinal level (Basbaum & Fields, 1984; Gautier et al., 2017; Heinricher et al., 2009; Lau & Vaughan, 2014; Zhuo & Gebhart, 1990).

Anatomical studies have shown that RVM projections to the dorsal horn of the spinal cord release either serotonin or the inhibitory neurotransmitters GABA and/or glycine (Hossaini et al., 2012; Marinelli et al., 2002; Pedersen et al., 2011; Zhang et al., 2015). Electron microscopy of RVM projection terminals in the SDH suggests that the majority of these terminals release GABA, with some also releasing glycine (Aicher et al., 2012; Antal et al., 1996; Light & Kavookjian, 1985) and these findings have been supported by an *in vivo* electrophysiological study (Kato et al., 2006). More recently, behavioural studies using opto- or chemogenetics to selectively engage inhibitory descending populations confirm that they modulate nocifensive responses and itch (Cai et al., 2014; Francois et al., 2017; Nguyen et al., 2022; Zhang et al., 2015). As a result, modulation of spinal nociception by RVM inputs into the SDH is thought to be primarily mediated by GABA, with a relatively minor contribution of glycinergic signalling.

Immunohistochemical studies show that GABAergic, parvalbumin-positive and non-GABAergic, calbindin-positive (presumably glutamatergic) SDH neurons receive inputs from the RVM (Aicher et al., 2012; Antal et al., 1996). These SDH target neurons appear to consist of several different morphological types (Kato et al., 2006; Light & Kavookjian, 1985). Furthermore, diverse populations of inhibitory RVM projections have also been reported to make axo-axonic contacts with primary sensory afferents (Zhang et al., 2015) and preproenkephalin-positive-inhibitory interneurons (Francois et al., 2017). Nevertheless, there is little consistent data about the SDH neurons targeted by descending inhibitory RVM projections and no study has comprehensively assessed it functionally.

Both spinal (sensory afferents, projection neurons and interneurons) and descending circuits are well known to contribute to the analgesic actions of opioids (Corder et al., 2018; Zorman et al., 1982), but the precise details as to how this is achieved are lacking. Intrathecal injection of mu (μ), kappa (κ) and delta (δ) opioid receptor agonists

© 2022 The Authors. *The Journal of Physiology* published by John Wiley & Sons Ltd on behalf of The Physiological Society.

(Bailey et al., 1993; Borgbjerg et al., 1996; Goodchild & Gent, 1992; Morgan et al., 1992; Schmauss, 1987) is generally analgesic, although the data for κ-agonists are somewhat inconsistent (Danzebrink et al., 1995; Kim et al., 2011). Within the SDH, opioid receptor activation inhibits excitatory synaptic currents (EPSCs), particularly those originating from primary sensory afferents (Gerhold et al., 2015; Glaum et al., 1994; Hori et al., 1992; Kim et al., 2018; Kohno et al., 1999; Randic et al., 1995; Snyder et al., 2018). In contrast, opioid modulation of inhibitory synaptic currents (IPSCs) has not been reliably observed (Grudt & Henderson, 1998; Kerchner & Zhuo, 2002; Kohno et al., 1999). Together these data suggest that within the SDH, opioids target excitatory transmission to a greater extent than inhibitory transmission. How the synapse between RVM axonal projections and their target neurons in the SDH contribute to opioid analgesia is unknown.

To address these gaps in knowledge, we combine optogenetics with *ex vivo* electrophysiology to selectively stimulate RVM projections and directly investigate their synaptic properties and target neurons within the SDH. Then, to better understand how opioids modulate this descending input, we determined the effects of μ-, κ- and δ-opioid receptor agonists at this synapse.

Methods

Ethical approval

Experiments were carried out on male and female Sprague Dawley rats in accordance with guidelines set by the National Health and Medical Research Council's Australian code of practice for the care and use of animals for scientific purposes and in accordance with the International Association for the Study of Pain (Washington, DC). All experiments were approved by the Northern Local Health District Animal Ethics Committee (Approval no. RESP18-208). Pregnant female rats were obtained from the Animal Resources Centre (Canning Vale, Australia) and were housed in the Kolling Institute Facility. After weaning, rats of the same gender were housed in groups of two to three in individually ventilated cages under controlled light (12-h light–dark cycles) and temperature (23 $\pm$ 1°C, 70% humidity) with *ad libitum* access to water and food pellets. Cages were enriched with a house igloo, tissues for nesting, and straws or paddle pop sticks on alternate weeks. A total of 73 male and 34 female rats were used in the study. The authors understand the ethical principles and verify that the work presented complied with the journal's ethical checklist.

Stereotaxic injection

Stereotaxic injections were performed on 3 to 4-week-old rats weighing 40–90 g under 1.5–3% isoflurane anaesthesia using a stereotactic apparatus (Kopf Instruments, Tujunga, CA, USA). An AAV8.Syn.ChR2 (H134R).GFP (3.3×10^{13} genomic copies/ml, a kind gift from Edward Boyden; Addgene no. 58880) or AAV5.hSyn.hChR2(H134R).mCherry.WPRE.pA (5.8×10^{12} genomic copies/ml; a kind gift from Karl Deisseroth; UNC Vectorcore av4320d) was injected through a glass capillary pipette (40–70 μm diameter) in the rostral ventromedial medulla (RVM) at an angle of 10° posterior to the target area to avoid the transverse venous sinus. The following coordinates were used: Bregma ML: 0.0 mm; AP, −8.3 to 10.1 mm; DV, −7.9 to 9.7 mm, scaled by the ratio of the measured bregma–lambda distance (6.8–8.3 mm) to the adult distance of 9 mm. Injections were delivered at a rate of 15 nl min^{-1} for a total volume of around 120 nl (Nanoject II, Drummond) and following the injection the pipette was left in place for 5 min, then slightly lifted (50 μm) and held in place for additional 10 min before complete removal. Animals were given post-operative analgesia (buprenorphine 0.05 mg kg^{-1}, I.P.) and carefully monitored until experiments were performed 7–10 weeks later.

Spinal cord slice preparation

Rats were deeply anaesthetised with isoflurane (3%, assessed by rate of breathing, lack of righting reflexes and lack of response to paw squeeze) and killed by exsanguination. Rats were transcardially perfused with ice-cold *N*-methyl-D-glucamine solution (NMDG) containing (in mM): 93 NMDG, 30 $NaHCO_3$, 25 glucose, 2 thiourea, 3 sodiumpyruvate, 2.5 KCl, 1.2NaH_2PO_4, 20 HEPES, 10 $MgSO_4$, 0.5 $CaCl_2$, 5 sodium ascorbate, 2 kynuenic acid (∼300 mOsm), equilibrated with 95% O_2–5% CO_2. Parasagittal spinal cord slices (280 mm) of the lumbar enlargement were prepared with a vibratome (Leica VT1200S) in the same ice-cold NMDG solution and then maintained in this solution for 10 min at 34°C. After, they were transferred into artificial cerebrospinal fluid (ACSF) (in mM: 126 NaCl, 2.5 KCl, 1.2 NaH_2PO_4, 1.2 $MgCl_2$, 2.4 $CaCl_2$, 11 glucose, and 25 $NaHCO_3$, equilibrated with 95% O_2 and 5% CO_2) and kept at room temperature (RT) until use.

Electrophysiology

For recording, slices were individually transferred to a chamber on an upright fluorescence microscope (Olympus BX51) and superfused continuously with ACSF (33°C, flow rate 2.5 ml min^{-1}). Spinal cord neurons were visualised with a 40× water-immersion objective using Dodt gradient contrast optics. SDH neurons were selected for recording from the clear band of the *substantia gelatinosa* (lamina II, see Fig. 1; Chery & De Koninck, 1999) if they had GFP-labelled RVM axons

© 2022 The Authors. *The Journal of Physiology* published by John Wiley & Sons Ltd on behalf of The Physiological Society.

near their soma. Lamina I projection neurons were not excluded from our recordings, but given the location of our recordings, their scarcity in the SDH (Polgar et al., 2010) and the firing patterns and morphologies we observed (Ruscheweyh et al., 2004), we do not consider that they were significantly sampled. Whole-cell patch-clamp recordings from these spinal cord neurons were performed in current-clamp or voltage-clamp configuration. Patch pipettes (3–5 MΩ) were filled with an intracellular solution composed of (mM): 136 potassium gluconate, 4 NaCl, 5 EGTA, 0.5 $CaCl_2$, 10 HEPES, 5 sodium phosphocreatine, 5 MgATP, 0.3 NaGTP, and 0.1% biocytin, pH 7.3 with KOH (290–295 mOsm). The chloride reversal potential using these solutions is ∼−87 mV. Series resistance (<25 MΩ) was compensated by 65% and continuously monitored during experiments. The liquid junction potential was not corrected. After determining the firing properties of each neuron, a brief blue laser light (0.5–1 ms, 473 nm; OptoDuet Laser, IkeCool, Los Angeles, CA, USA) was delivered at 20–30 s intervals through the objective lens (40×) of the microscope to illuminate the superficial laminae of the dorsal horn. Only SDH neurons that displayed light-activated currents are reported (∼10% of neurons tested) and only one cell was recorded from each slice. Inhibitory postsynaptic currents (oIPSCs) were outward under our recording conditions and were pharmacologically isolated in the presence of the AMPA/kainate receptor antagonist 6-cyano-7-nitroquinoxaline-2,3-dione (CNQX, 10 μM) or 2,3-dioxo-6-nitro-1,2,3,4-tetrahydrobenzo[*f*]quinoxaline-7-sulfonamide (NBQX, 5 μM) and the NMDA receptor antagonist D-2-amino-5-phosphonopentanoic acid (D-AP5, 25 μM). The $GABA_A$ receptor antagonist SR95531 (3 μM) and the glycine receptor antagonist strychnine (0.5 μM) were added to isolate the glycine- and $GABA_A$-receptor mediated currents. Specificity of opioid receptor-mediated actions were ensured by determining whether agonist effects reversed by the relevant specific antagonist. All recordings were filtered (4–10 kHz low pass filter) with Multiclamp 700B amplifier (Molecular Device) and digitised at a sampling rate of 10 kHz with an A/D converter (NI USB-6251, National Instruments) and stored using a data acquisition program (AxographX, Axograph Scientific Software). Off-line analysis was performed using Clampfit10 (Molecular Device) and Igor Pro 6 (WaveMetrics).

Immunohistochemistry and confocal imaging

Rats were deeply anaesthetised by isoflurane or intraperitoneal injection of pentobarbital sodium 80 mg kg^{-1}) and perfused transcardially with NMDG solution or 4% paraformaldehyde (PFA) in 0.1 M phosphate buffered saline (PBS). Brains and spinal cords were removed and post-fixed in 4% PFA for 48 h at 4°C. Coronal sections of the brainstem (40–80 μm thick) and parasagittal sections of the lumbar spinal cord (40–280 μm thick) were cut with a vibratome (Leica VT100S). Free-floating sections were rinsed in PBS, incubated in 50% ethanol for 30 min, and then for 3 h in PBS supplemented with 0.3% Triton X-100% and 10% horse serum. They were then incubated for 48 h at 4°C with goat polyclonal CGRP antibody (1:1000, Abcam, Cambridge, UK), biotinylated lectin IB4 (1:500, Invitrogen) and chicken polyclonal GFP antibody (1:1000, Aves lab) diluted in PBS supplemented with 0.1% Triton X-100% and 10% horse serum. They were then rinsed in PBS and incubated for 3 h at room temperature with donkey anti-goat Alexa-568 (1:1000, Abcam), streptavidin Alexa-647 (1:1000, Abcam) and donkey anti-chicken Alexa-488 (1:1000, Jackson Immuno Res). Negative controls without the addition of the primary antibody were carried out. To visualise biocytin-filled cells following electrophysiological recording, spinal cord slices were fixed in 10% formalin solution (Sigma, Sydney, Australia) and incubated with streptavidin Alexa-647 (1:1000, Abcam). Sections and slices were rinsed in PB, mounted with Mowiol/Dabco (25 mg ml^{-1}) and stored at 4°C. All sections were imaged in a Leica TCS SP5 confocal microscope using a 20× (NA 0.7) or a 40× (NA 1.25) objective and Ar/Kr laser set at 488, 561 and 633 nm for excitation of Alexa-488, Alexa-568 and Alexa-647, respectively. Stacks of optical sections were acquired at a pixel resolution of 0.12 μm and a z-step ∼1 μm, and images were processed using ImageJ software (NIH). SDH cell morphology was classified based on previously described criteria (Yasaka et al., 2010). Briefly, islet cells have an extensive rostrocaudal (RC) dendritic tree spanning >400 mm and small dorsoventral (DV) dendritic trees. Central cells have a similar form, but their RC dendritic trees are shorter. Radial cells have similar length dendrites in RC and DV directions and the largest soma to dorsal (SD) dendritic tree length. Vertical cells have dominant ventral dendrites and short dorsal dendrites, resulting in a distinct SV/SD ratio (Table 1).

Both male and female rats were used in all experimental groups and additional animals were added to several experiments where the analysis was based on neuronal type, as this could only be determined following *post hoc* visualisation.

Neuron properties procedures

Neuron electrical properties. Resting membrane potential (RMP) was monitored in the current-clamp configuration ($I = 0$ mode) immediately after entering whole-cell mode. Action potential (AP) discharge patterns were obtained by injecting 20 pA step currents of 1 s duration ranging from −100 to 300 pA at 5 s interval. Membrane resistance (R_m) was calculated from responses

© 2022 The Authors. *The Journal of Physiology* published by John Wiley & Sons Ltd on behalf of The Physiological Society.

Table 1. Morphological dimensions of dendritic trees

	n	RC	DV	RC/DV	SD	SV	SV/SD
Islet†	3	**423 ± 12**	75 ± 40	6.7 ± 2.9	38 ± 18	37 ± 23	1.0 ± 0.2
Central	6	225 ± 112	**65 ± 26***	3.6 ± 2.3	22 ± 15	**44 ± 18***	2.7 ± 2.0
Radial	7	184 ± 42	145 ± 34	**1.3 ± 0.5***	**61 ± 18***	84 ± 26	1.5 ± 0.6
Vertical	12	267 ± 91	129 ± 30	2.1 ± 0.7	21 ± 10	109 ± 24	**6.5 ± 3.7***

Values shown are the means ± SD (μm). Data are from the $n = 28$ classifiable target SDH neurons from $n = 24$ rats. Abbreviations: RC, rostocaudal; DV, dorsoventral; RC/DV, ratio of rostocaudal to dorsoventral; SD, soma central to dorsal end; SV, soma central to ventral end. Bold indicates a dimension that helps to distinguish cell types. Statistical differences were assessed using two-tailed one-way ANOVA with Tukey and Kruskal-Wallis test with Dunn-Bonferroni. Significant difference in dimensions compared to other morphology types is indicated (*$P < 0.05$). Complete statistical information is presented in the Statistical Summary Document. †See Discussion.

in the linear region of current-voltage relationship around RMP. AP discharge patterns were classified based on previously described criteria (Abraira et al., 2017; Grudt & Perl, 2002; Santos et al., 2004). Briefly, Delayed-firing (DF) neurons showed a ramped and delayed potential preceding AP discharge: Tonic-firing (TF) neurons showed a continuous firing pattern; Phasic-firing (PF) neurons showed similar characteristics to TF neurons, except they displayed burst firing ($\geq$ 2 AP, 30–150 Hz) at rheobase potential; Adapted-firing (AF) neurons showed several APs during the early period in the depolarisation step. Gap-firing (GF) neurons showed a clear gap between bursts of APs. The classification of AP discharge was determined within 5 min after whole-cell mode since changes in the cells intracellular environment can affect AP frequency and adaptation (Prescott & De Koninck, 2002). For our analysis, we classified neurons into two groups, DF or non-DF (AF, PF, TF).

oIPSCs and drug responses. Patch clamped SDH neurons were monitored in voltage-clamp mode at a membrane potential of −50 mV. If a current of more than 10 pA was detected in response to a brief pulse of blue light, the laser power or duration (max. 1 ms) was increased until a 50–1200 pA oIPSC current was stimulated (291 ± 224 pA, $n = 146$). After the baseline stabilised, (>5 min) experiments to investigate drug effects were commenced. Drugs were applied 5–10 min and a minimum of 6 traces (>2 min period) were averaged to measure the amplitude, PPR and decay time constant of oIPSCs in the absence or presence of drugs. Drug effects on oIPSCs were assessed at fixed time points: over the last 2 min prior to drug application, during drug application and then during washout or antagonist application. The glycinergic contribution to oIPSCs was measured as the amplitude of the oIPSC remaining following application of SR95531, or as the decrease in oIPSC amplitude after strychnine application. Decay time constants were measured by fitting a bi-exponential function to the averaged oIPSC, and a weighted decay time constant was calculated using the function in pClamp 10.

Opioid agonist experiments. After the baseline stabilised, (>5 min) experiments to investigate drug effects were commenced. The opioid receptor-specific actions of μ, δ and κ agonists on SDH target neurons were confirmed if their effects were reversed by the relevant opioid receptor-specific antagonist. In experiments comparing opiate receptor agonists' effects on oIPSCs, between 1 and 3 different opioid agonists were tested in each neuron according to established protocols (Lau et al., 2020; Winters et al., 2017). The experimenter randomly rotated the order of drug application between different recordings to reduce potential bias resulting from the order of drug testing and ensure specific drug experiments were carried out across different animals. The percentage effects of opioid agonists on oIPSC parameters were calculated as the value measured during opioid agonist application divided by the average of the pre-agonist and washout-in-antagonist values. Thus, in cells where sequential opioid agonist/antagonist combinations were tested, the pre-agonist value was measured in solution with other opioid-related agonists and their specific antagonists present (Lau et al., 2020; Winters et al., 2017). Cells were defined as opioid inhibited/responders if a significant decrease in the oIPSC amplitude was observed after the agonist application (Mann-Whitney test) which partially or fully recovered in the presence of its specific antagonist. Otherwise, they were defined as non-inhibited/non-responders (see Fig. 7).

Paired photostimulation (50 ms interval) was used to calculate the paired-pulse ratio (PPR), the ratio of the second oIPSC peak amplitude over the first peak amplitude. We verified that PPR changes reflect pre- and postsynaptic drug effects at this synapse by measuring the PPR effects of antagonists of postsynaptic $GABA_A$ or glycine receptors, or the agonist of presynaptically

© 2022 The Authors. *The Journal of Physiology* published by John Wiley & Sons Ltd on behalf of The Physiological Society.

expressed $GABA_B$ receptors (Yang et al., 2002) (see Fig. 7*E*–*G*).

Drug effects on SDH-target neuron holding currents. The holding current was measured by averaging the entire recording period (5–20 s) outside of each photostimulation episode. Postsynaptic currents in response to opioid agonists application were filtered offline (50 Hz low-pass filter) for analysis. A neuron was considered to have a holding current response to an agonist if it produced an outward current of >6 pA during continuous agonist superfusion that reversed upon application of the appropriate antagonist (Pedersen et al., 2011).

Drugs and reagents

All reagents were obtained from Sigma-Aldrich, Abcam and Tocris Bioscience (Bristol, UK). Opioid-related drugs were as follows; [5-methionine] enkephalin (10 μM; Sigma), [D-Ala^2, NMe-Phe^4, Gly-ol5]-enkephalin (DAMGO, 1 μM; Abcam) and antagonist D-Phe-Cys-Tyr-D-Trp-Arg-Thr-Pen-Thr-NH_2 (CTAP, 1 μM; Abcam), U69593 (0.3 μM; Abcam) and antagonist nor-binaltorphimine (nor-BNI, 0.3 μM; Abcam), [D-Ala^2]-deltrophin II (0.3 μM; Abcam) and antagonist ICI174864 (1 μM; Tocris). Stock solutions of neurochemicals were made in distilled water, or DMSO, aliquoted and then frozen. Stock solutions of neurochemicals were made in distilled water, or DMSO, aliquoted and then frozen. During recordings, stock drugs were diluted to working concentrations in ACSF ($\leq$1:3000 drug solvent: ACSF) immediately before use and applied by bath superfusion.

Statistics

All data are expressed as means ± SD (error bars). Statistical analysis was undertaken only for data sets where group size $\geq$5 with IBM SPSS statistics version 26. Normality was assessed with Shapiro-Wilk test and no significant variance inhomogeneity was confirmed with Levene test or Mauchly's test. Data from male and female rats were grouped as no significant sex differences were noted (see Fig. 9). We used parametric statistics and *post hoc* tests (two-tailed Student's *t* test, one-way ANOVA with Tukey or repeated measure ANOVA with Bonferroni) if the data distribution was normal and variability homogenous. *Post hoc* tests were conducted only if *F* achieved $P < 0.05$. In cases where these requirements were not met, non-parametric statistics and *post hoc* tests were used (Friedman test with Dunn-Bonferroni, Kruskal-Wallis test with Dunn-Bonferroni, Wilcoxon signed-rank tests and Mann-Whitney test). Differences were considered significant when $P < 0.05$.

Results

RVM projections to the spinal cord dorsal horn terminate primarily in LI-LIIo and are inhibitory

To examine synaptic transmission from the rostral ventromedial medulla (RVM) onto neurons in the superficial dorsal horn (SDH), we injected an adeno-associated viral vector (AAV) encoding channelrhodopsin-2 (ChR2) fused to green fluorescence protein (GFP) into the RVM (Fig. 1*A*). ChR2/GFP positive (ChR2$^+$/GFP$^+$) fibres were detected in superficial and deep laminae of the spinal

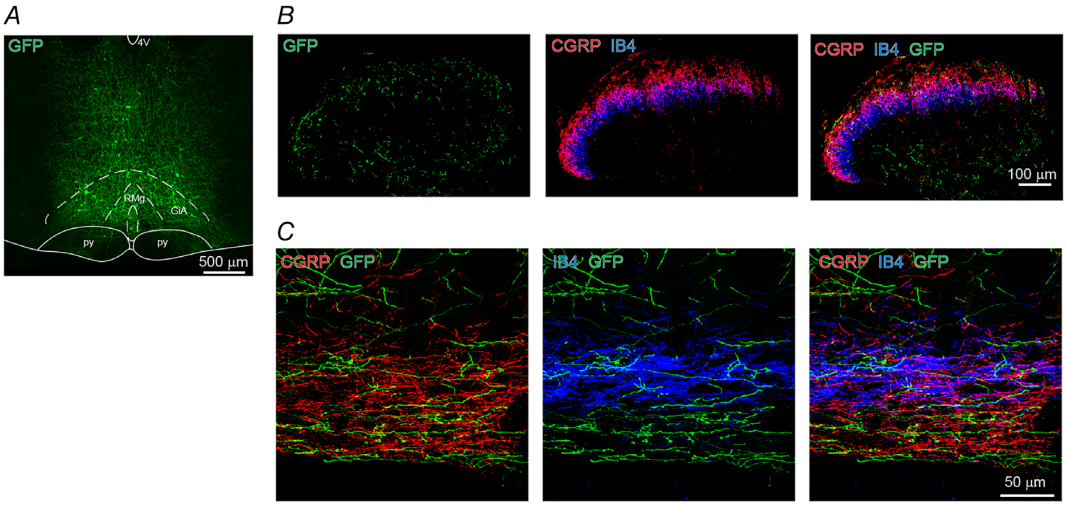

Figure 1. RVM projections terminate primarily in LI-LIIo of the SDH
A, GFP expression in RVM neurons. Coronal (*B*) and parasagittal (*C*) section of spinal cord dorsal horn from a rat injected with AAV-ChR2-GFP (green) in the RVM. CGRP (red)- and IB4 (blue)-positive fibres are co-immunostained. RMg, raphe magnus nucleus; GiA, gigantocellular reticular nucleus (alpha part); py, pyramidal tract; 4V, fourth ventricle, replicated in seven rats. [Colour figure can be viewed at wileyonlinelibrary.com]

© 2022 The Authors. *The Journal of Physiology* published by John Wiley & Sons Ltd on behalf of The Physiological Society.

dorsal horn (Fig. 1*B*). Because nociceptive and thermoreceptive Aδ and C afferents terminate largely in lamina I and II (Todd, 2010), we focused our attention on the SDH. Here, ChR2$^+$/GFP$^+$ fibres were predominantly present in lamina I (LI) and outer lamina II (LIIo) as identified by calcitonin gene-related peptide (CGRP) expression, but less so in inner lamina II (LIIi) as identified by isolectin B4 (IB4) expression (Fig. 1*B, C*; $n = 7$ rats). This innervation pattern is consistent with previous reports (Antal et al., 1996).

In parasagittal spinal cord slices, SDH neurons were patch clamped in whole-cell voltage clamp mode at a holding potential of −50 mV (Cl^- equilibrium potential = −87 mV) and synaptic currents were monitored when ChR2$^+$/GFP$^+$ fibres were excited with blue light. Optical stimulation evoked reliable outward currents (Fig. 2*A*) with no failures and, unlike spontaneous inward synaptic currents, the optically evoked postsynaptic currents were unaffected by the AMPA and NMDA receptors antagonists NBQX and APV (Fig. 2*A* and *B*, $n = 10$ cells from eight rats). However, they were blocked by co-application of the $GABA_A$ and glycine receptor antagonists SR95531 and strychnine. Together these data demonstrate that light activated currents are inhibitory GABA and glycine synaptic currents (oIPSCs; Fig. 2*A* and *B*) resulting from monosynaptic input from RVM projection fibres. A monosynaptic connection is supported by control experiments showing that oIPSCs were abolished by the voltage gated sodium channel blocker TTX and recovered by addition of the potassium channel blocker 4-AP (Fig. 2*C* and *D*) (Petreanu et al., 2009).

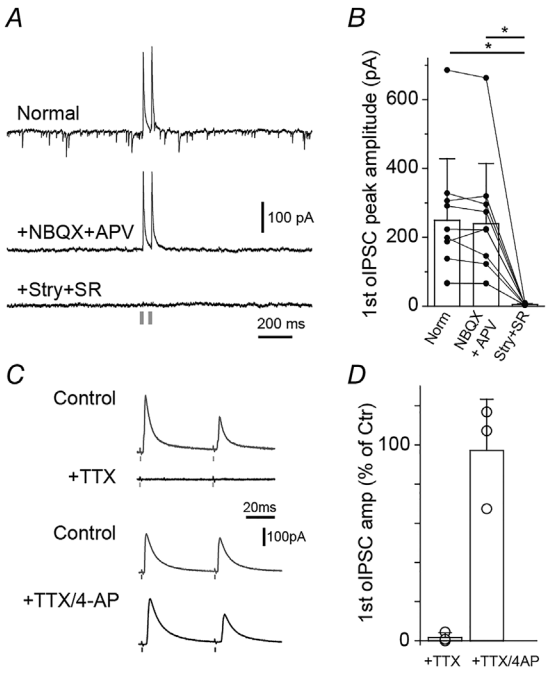

Figure 2. Optogenetic activation of RVM projections stimulate GABA/glycine IPSCs
A, pairs of light-stimulated currents evoked in SDH target neurons voltage clamped at −50 mV. Inward currents were blocked by NBQX and D-APV (middle). Outward currents were blocked by strychnine and SR95531 (bottom) indicating optically evoked currents are inhibitory postsynaptic currents (oIPSCs). *B*, bar graph of antagonist effects on the peak amplitude of the first light-stimulated current of $n = 10$ cells from eight rats ($P > 0.0001$ (Norm *vs*. Stry+SR) and 0.011 (NBQX+APV *vs*. Stry+SR); Friedman test with Dunn-Bonferroni *post hoc* test). *C*, oIPSCs were suppressed by the presence of the voltage-gated sodium channel blocke tetrodotoxin (TTX, 0.5–1 μM, $n = 3$) and this effect was prevented by adding potassium channel blocker 4-aminopyridine (4-AP, 100 μM, $n = 3$; Petreanu et al., 2009). *D*, quantification of *C*.

Properties of SDH neurons targeted by the inhibitory RVM input

SDH neurons have been classified by their electrophysiological and morphological properties in rodents (Grudt & Perl, 2002; Yasaka et al., 2010; but see Browne et al., 2020). To characterise SDH neurons that receive oIPSCs, we analysed their AP firing pattern in response to depolarising currents, membrane properties (input resistance (R_m) and resting membrane potential (RMP)) ($n = 77$ cells from 59 rats), plus their morphological features ($n = 42$ cells from 36 rats, *post hoc* biocytin staining). SDH neurons which received inhibitory RVM inputs were primarily delayed- (DF; 44%) and tonic-firing (TF; 38%) neurons, although phasic- (PF), adapted- (AF) and gap-firing (GF) action potential firing patterns were also observed (Fig. 3*A* and *B*). Membrane properties were similar amongst these cell types, except for PF neurons which had a more depolarised RMP (Fig. 3*C*; $P > 0.0001$ (DF *vs*. PF); $P > 0.0001$ (TF *vs*. PF); two-tailed one-way ANOVA with Tukey *post hoc* test).

Morphological analysis, based on four defined dendritic tree shapes (islet, vertical, radial and central) (Browne et al., 2020; Grudt & Perl, 2002; Yasaka et al., 2010) was conducted in SDH target neurons with either a DF or TF firing pattern, as these are the major target of RVM projections ($n = 42$ cells from 36 rats). Two-thirds of DF and TF SDH target neurons were classified into one of four defined types ($n = 28/42$, Fig. 4*A–J* and Table 1) and the remaining one-third were unclassifiable ($n = 14/42$ cells, Fig. 4*K–M*). The morphologies of DF and TF neurons were investigated in more depth. All morphological types were found in the TF neuronal population. DF neurons had all morphologies except islet cells and there were more radial DF- than TF-neurons (Fig. 4). However, no significant difference in morphological properties between TF and DF neurons were detected ($P = 0.177$, Fisher's exact test).

© 2022 The Authors. *The Journal of Physiology* published by John Wiley & Sons Ltd on behalf of The Physiological Society.

Optically evoked IPSCs have both GABAergic and glycinergic components

Stimulation of the RVM projection can induce GABAergic and/or glycinergic responses in SDH neurons (Hossaini et al., 2012; Kato et al., 2006). We assessed the relative contribution of GABA and glycine to oIPSCs by applying strychnine ($n = 18$ from 17 animals) or SR95531 ($n = 17$ cells from 14 animals). Each antagonist reduced the amplitude and changed the decay kinetics of oIPSCs (Fig. 5*A* and *B* and 2*B*). The decay kinetics of the SR95531-insensitive glycinergic oIPSCs were faster than strychnine-insensitive GABAergic oIPSCs (Fig. 5*B*, $P < 0.0001$, two-tailed unpaired t test), consistent with previous reports (Anderson et al., 2009; Labrakakis et al., 2014). Moreover, we found that oIPSCs with faster decay kinetics had a larger glycinergic component (Fig. 5*C*; $R^2 = 0.288$, linear regression analysis) and noticed that DF neurons had a larger percentage glycine component compared to TF, PF, AF and GF (non-DF) types (Fig. 5*C*; glycinergic component of DF cells (green circles) = 69.1 ± 23%, $n = 14$ from 13 rats *vs*. non-DF (orange circles) = 50.6 ± 20%, $n = 21$ from 17 rats, $P = 0.017$, two-tailed unpaired t test). When we compared the decay of DF neurons ($n = 24$ cells from 19 animals) to that of non-DF neurons ($n = 36$ neurons from 32 rats; Fig. 5*D* and *E*) we found that the decay kinetics of oIPSCs in DF neurons were faster than other neuron types (Fig. 5*D* and *E*; $P = 0.001$ (DF *vs*. TF), $P = 0.004$ (DF *vs*. PF), Kruskal-Wallis test with Dunn-Bonferroni *post hoc*) suggesting DF neurons receive a glycine dominant descending input from the RVM.

Kappa- and mu-opioid receptor agonists inhibit signalling at the RVM-SDH synapse

While there is much evidence that opioids modulate spinal nociceptive circuits by modifying excitatory neurotransmission (Hori et al., 1992; Kohno et al., 2003; Kumamoto et al., 2011; Yaksh, 1987), less is known about their actions on inhibitory transmission. To determine if opioids modulate the inhibitory synapse formed between descending RVM inputs and their SDH target neurons, we compared the effect of μ-, κ- and δ-opioid receptor agonists on pairs of oIPSCs (Fig. 6). It was observed that the amplitude of oIPSCs in most SDH target neurons were inhibited by the κ-agonist U69593, some were inhibited by the μ-agonist DAMGO, and none were altered by the δ-agonist deltorphin II (Fig. 6*A*–*E*, $n = 34/41$, 17/38,

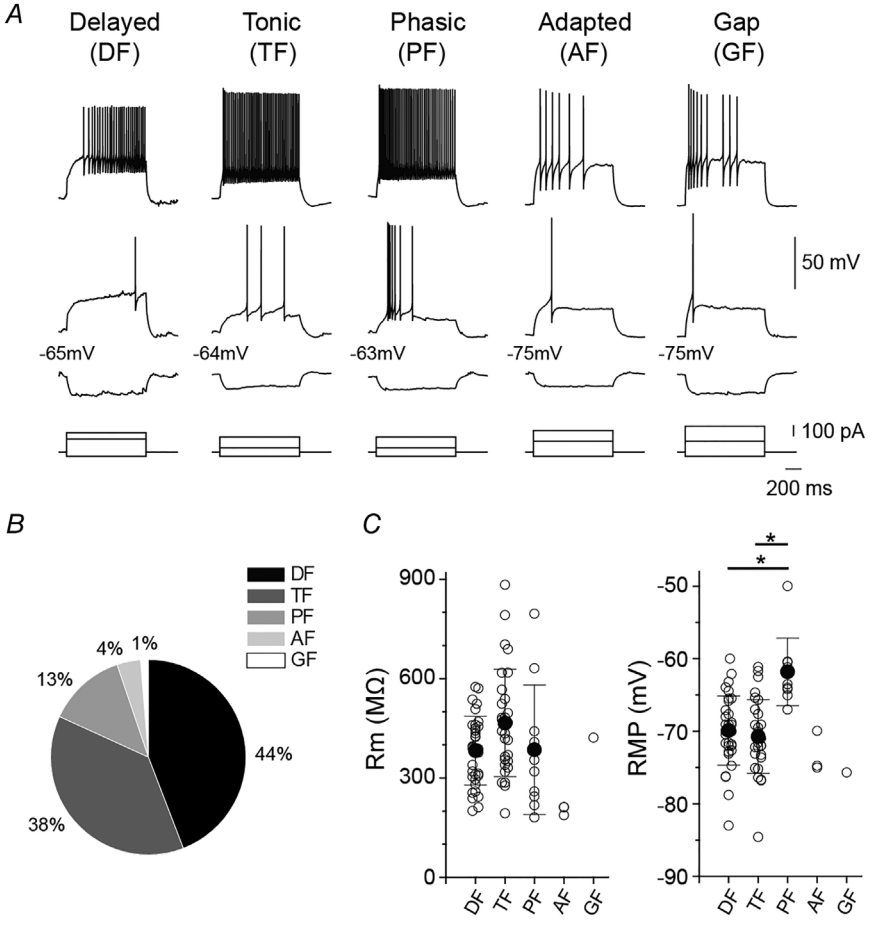

Figure 3. oIPSCs were detected in different types of SDH-target neurons
A, example AP discharge patterns of SDH target neurons receiving oIPSCs. APs induced by somatic injection of hyperpolarizing, rheobase and depolarizing current (1 s duration) are shown. *B*, pie chart summarizing AP discharge patterns ($n = 77$ SDH target neurons from 59 rats). *C*, membrane resistance (R_m) and resting membrane potential (RMP) in DF ($n = 34$), TF ($n = 29$), PF ($n = 10$), AF ($n = 3$), and GF ($n = 1$) neurons; (RMP: $P = 0.778$ (DF *vs*. TF), $P > 0.0001$ (DF *vs*. PF), $P > 0.0001$ (TF *vs*. PF), two-tailed one-way ANOVA with Tukey *post hoc* test). All data shown are means ± SD.

© 2022 The Authors. *The Journal of Physiology* published by John Wiley & Sons Ltd on behalf of The Physiological Society.

1/20). The effects of U69593 and DAMGO were selectively reversed by the μ-, κ-receptor antagonists CTAP and nor-BNI, respectively, while the δ-antagonist ICI174864 had no effect (Fig. 6*A*–*D*). In 22 neurons where both μ- and κ-opioid agonists were tested in the same cell, the seven neurons that responded to DAMGO also responded to U69593.

We analysed the effects of opioid receptor agonists at DF and non-DF neurons. oIPSCs were inhibited in a greater portion of DF-neurons by U69593 compared to DAMGO (81%, $n = 13/16$ for U69593 *vs.* 23%, $n = 3/13$ for DAMGO, $P < 0.05$ Fischer's exact test; Figs 6*D* and *E* and 7*A* and *C*). By contrast, U69593 and DAMGO inhibited a similar proportion of oIPSCs at non-DF neurons (84%, $n = 21/25$ for U69593; 56%, $n = 14/25$ for DAMGO, $P = 0.06$ Fischer's exact test; Figs 2*D* and *E* and 7*B* and *D*).

Opioid agonists presynaptically inhibit the RVM to SDH synapse

The effect of opioid receptor agonists on the short-term plasticity characteristics of the RVM-SDH synapse was assessed to determine if opioid agonists are likely to act at the pre- or postsynaptic terminals (Fig 7*E*–*G*; Fioravante & Regehr, 2011). We measured the paired-pulse ratio (PPR) before and after drug application and during drug reversal with receptor-specific antagonist (Fig. 6*F* and *G*). Responses to U69593 and DAMGO were accompanied by a change in PPR, indicating κ- and μ-receptor agonists have a pre-synaptic mode of action. On the other hand, the PPR did not change in the presence of deltorphin II (Figs 6*A*–*F*,*G* and 7*A*–*D*).

A subset of SDH target neurons have opioid-induced postsynaptic responses

Under our recording conditions, DAMGO, deltorphin-II and U69593 induced outward currents in some SDH target neurons (Figs 6*A*–*C* and 8). These outward currents, probably opioid-induced potassium channel currents, were reversed by CTAP, ICI174864 and nor-BNI, respectively (Figs 6*A*–*C* and 8) (Eckert & Light, 2002; Kim et al., 2018; Santos et al., 2004; Wang et al., 2018). Postsynaptic currents in response to DAMGO (62.5 ± 60.8 pA, $n = 33/56$ neurons) and deltorphin II (18.2 ± 12.5 pA, $n = 10/26$ neurons) were commonly detected, while small U69593 stimulated currents were measured in a minority of SDH neurons (10.5 ± 3.4 pA, $n = 9/49$ neurons; Fig. 8*A*–*D*). When we assessed the postsynaptic opioid effects at DF and non-DF subgroups of neurons, we found that DAMGO induced larger and more frequent currents in non-DF neurons than DF neurons (Fig. 8*C* and *D*). Similar holding current results were observed when the endogenous μ/δ-opioid receptor agonist met-enkephalin, was applied (not shown).

Recently, a small population of excitatory lamina II SDH neurons (10%) have been shown to co-express μ- and δ-opioid receptors (Wang et al., 2018). We analysed 20 neurons where both deltorphin II and DAMGO was applied. Postsynaptic DAMGO responses were measured in the majority of SDH target cells that responded to deltorphin II (6/7 neurons; Fig. 8*E*–*G*).

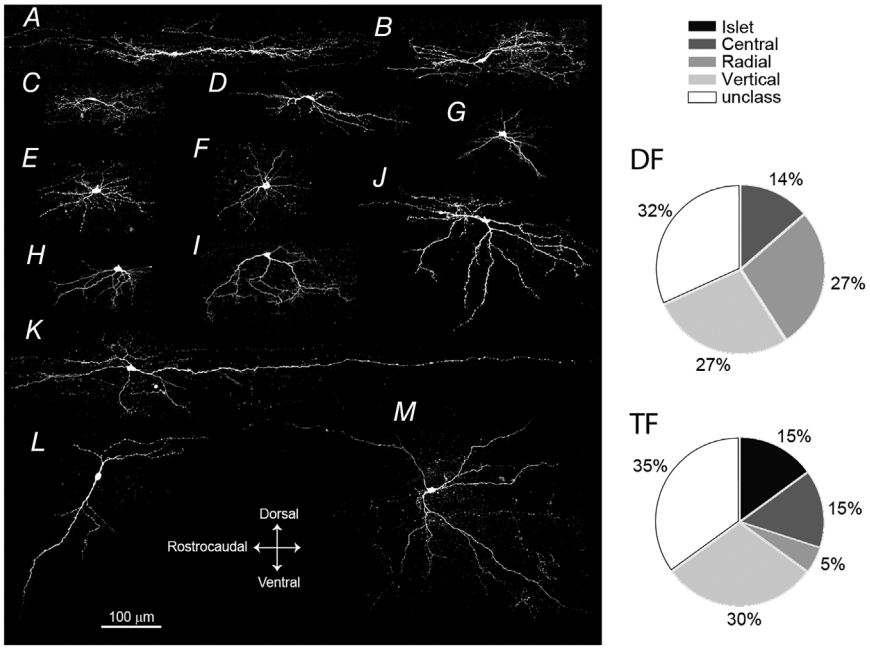

Figure 4. Morphology of RVM-SDH target neurons confocal images of biocytin-filled SDH target neurons
Cells were classified as islet cell (*A*), central cells (*B*–*D*), radial cells (*E*–*G*), vertical cells (*H*–*J*), and unclassified cells (*K*–*M*). Pie charts of cell morphology classifications from DF (22 cells) and TF (20 cells) neurons. No significant difference in morphological proportions between DF and TF neurons were detected ($n = 42$ cells from 36 rats; $P = 0.177$, Fisher's exact test).

© 2022 The Authors. *The Journal of Physiology* published by John Wiley & Sons Ltd on behalf of The Physiological Society.

Opioid agonist effects at the RVM to SDH synapse are similar in male and female rats

As the function of the descending pain pathway and response to opioids have significant sex differences (Custodio-Patsey et al., 2020; Loyd & Murphy, 2014; Mogil, 2020; Yu et al., 2021) we compared the data derived from male and female spinal slices. The opioid effects we described were similar in spinal tissue from female and male rats with respect to their effects on peak oIPSCs amplitude, PPR (Fig. 9*A* and *B*) and postsynaptic current (Fig. 9*C* and *D*).

Discussion

We have characterised the final synapse of a key descending pain modulatory pathway by selectively activating RVM projections into the SDH with optogenetics and investigated its modulation by opioids. We showed that stimulation of RVM projections into the SDH are inhibitory employing both GABAergic and glycinergic neurotransmission (we never observed excitatory or serotonergic currents), make connections with a highly heterogeneous population of SDH interneurons, and define a subgroup of DF neurons that receive oIPSC with a dominant glycinergic phenotype. Then, we improve our mechanistic understanding of how opioid mediated spinal analgesia is achieved by determining which opioids modulate the RVM to SDH synapse. We found that κ-opioid and to a lesser extent μ -opioid agonists presynaptically reduced oIPSCs in the SDH and detected a variable postsynaptic opioid agonist response. A comparison of opioid effects at DF and non-DF neurons suggests that these two types of connections are also differentially modulated. Together, these data enhance our knowledge of how descending inhibition to the SDH contributes to the processing of spinal sensory signals and the mechanisms fundamental to opiate mediated analgesia. These findings are essential building blocks for understanding spinal analgesia (endogenous and exogenous) and developing better alternatives to current opioid analgesics.

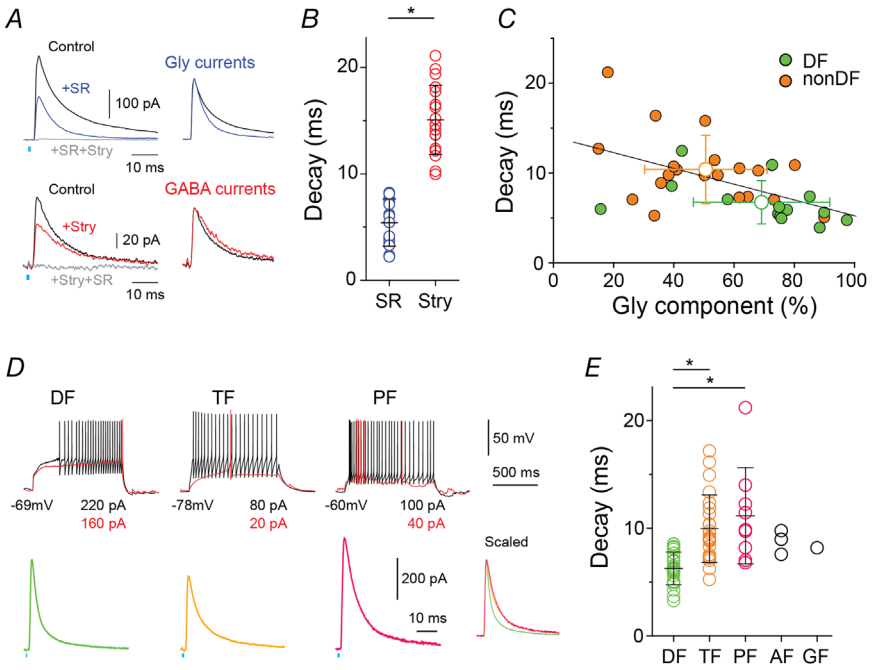

Figure 5. The oIPSC of DF neurons have a larger glycinergic component that non-DF neurons
A, the glycinergic and GABAergic components of oIPSCs were isolated by applying SR95531 and strychnine, respectively. Glycinergic oIPSCs (blue) had faster decay time constants than GABAergic (red) and control (black) oIPSCs. Co-application of both strychnine and SR95531 (grey) completely inhibited oIPSCs (3.6 ± 2.5% of control). Right, glycinergic and GABAergic currents normalised to their peak amplitude. *B*, quantification of decay time constant of oIPSC in the presence of SR95531 (blue, n = 17 from 14 rats) or strychnine (red, n = 18 from 17 rats; $P < 0.0001$, two-tailed unpaired t test). *C*, relationship between glycinergic component and decay time constant of the oIPSC under control conditions (n = 14 DF and 21 non-DF neurons; linear regression, $R^2 = 0.288$). *D*, control oIPSC examples from three types of SDH neurons classified by AP discharges during somatic injection of rheobase (red) and depolarising (black) currents. Right insert: oIPSC current from DF, TF and PF neurons normalised to their peak amplitude. *E*, comparison of decay time constants of control oIPSCs of neurons classified based on their firing pattern (DF: n = 24, TF: n = 23, PF: n = 9, AF: n = 3, GF: n = 1; P = 0.001 (DF *vs.* TF), P = 0.004 (DF *vs.* PF), Kruskal-Wallis test with Dunn-Bonferroni *post hoc* test). Mean ± SD are shown in *B*, *C* and *E*. [Colour figure can be viewed at wileyonlinelibrary.com]

© 2022 The Authors. *The Journal of Physiology* published by John Wiley & Sons Ltd on behalf of The Physiological Society.

Characterisation of the inhibitory GABA/glycine projections of RVM to SDH neurons

While descending inputs into the spinal cord are important modulators of spinal nociceptive processing, little was known about the relative glycine/GABA contribution to signalling or the spinal neurons they target (Lau & Vaughan, 2014; Ossipov et al., 2014; WeiWei et al., 2021). Data addressing these questions were incomplete, mainly because the roles and organisation of both the spinal circuit and the descending inputs are very complex and involve many different neuronal subtypes (Gautier et al., 2017; Haring et al., 2018; Todd, 2017). In addition, the tools needed to selectively activate specific inputs are relatively new, and the connections in the cord sparse; about 10% of our attempts to record oIPSCs in SDH neurons were successful.

SDH neuronal populations have long been differentiated by their electrical, morphological and neurochemical characteristics (Light & Kavookjian, 1985;

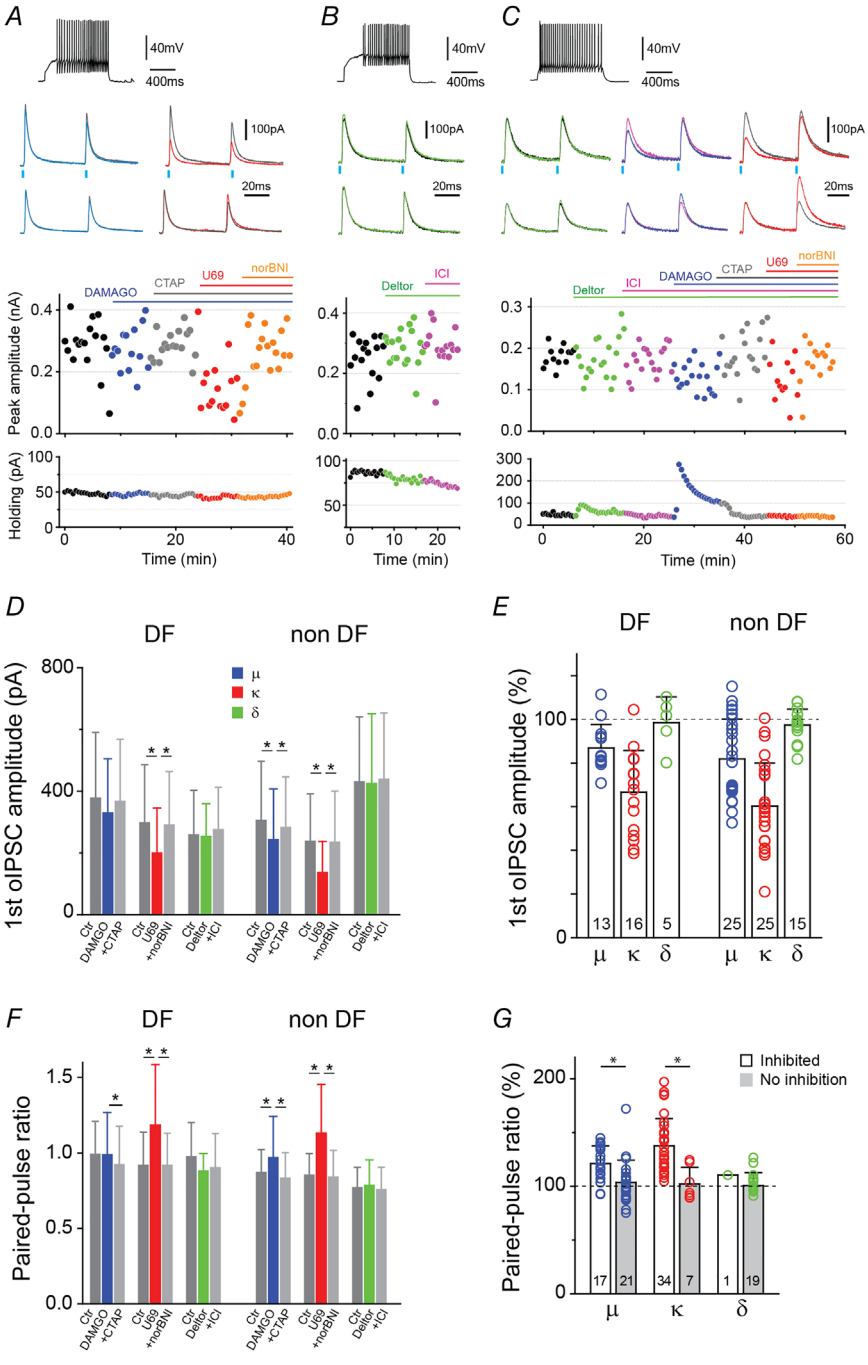

Figure 6. Mu- and kappa-, but not delta-opioid agonists inhibit oIPSCs
A, the μ- and κ-opioid agonists presynaptically inhibit oIPSCs. *A–C*, top: example of an AP discharge from DF (*A* and *B*) and non-DF (TF; *C*) neurons. Middle: superimposed oIPSCs pairs traces (top) and normalised traces to the 1st oIPSC peak (bottom) before and during opioid receptor agonists application. μ- (DAMGO, blue), κ- (U69593, red) and δ- (deltorphin II, green) opioid receptor agonists effects on oIPSC amplitudes and paired-pulse ratio (PPR) were confirmed by subsequent application of their corresponding antagonists, CTAP (grey), nor BNI (orange) and ICI174864 (green), respectively. Bottom: time plots of peak oIPSC amplitude (1st current) and the holding currents of SDH neurons, when opioid agonists/antagonists were applied. Bars indicate the time and duration of drug applications. *D*, summary of the peak amplitude effects of opioid receptor agonists followed by their specific antagonist on DF and non-DF neurons. Repeated measures ANOVA with Bonferroni; $F(2,24) = 3.952$ (μ, DF), $F(2,8) = 0.571$ (δ, DF), $F(2,28) = 0.664$ (δ, non-DF) and Friedman test with Dunn-Bonferroni. *E*, quantification of the percentage opioid agonist effects on oIPSCs peak amplitude in the same DF and non-DF neurons in D. *F*, summary of PPR effects of opioid receptor agonists followed by their specific antagonist on DF and non-DF neurons. Repeated measures ANOVA; $F(2,8) = 0.534$ and (δ, DF) and Friedman test with Dunn-Bonferroni. *G*, quantification of the percentage opioid agonist effects on PPR when neurons were divided into oIPSCs that inhibited (open bars; Mann-Whitney test, $P < 0.05$) or showed no response (grey bars; Mann-Whitney test, $P > 0.05$) to opioid agonists. In *E* and *G*, individual data points (open circles) and the total number of cells treated with agonist are indicated. All data shown are means ± SD. [Colour figure can be viewed at wileyonlinelibrary.com]

© 2022 The Authors. *The Journal of Physiology* published by John Wiley & Sons Ltd on behalf of The Physiological Society.

Yasaka et al., 2010). Recently, attempts to integrate these findings using non-biased characterisations of dorsal horn neurons have shown that none of the currently employed methods can be reliably linked to function (Browne et al., 2020; Merighi, 2018; Punnakkal et al., 2014; Smith et al., 2015; Todd, 2017). Despite this, there is a reasonable tendency for TF neurons, and neurons with an islet morphology, to be GABAergic and many DF neurons, especially large ones with a vertical neurite morphology, are glutamatergic (Browne et al., 2020; Merighi, 2018; Punnakkal et al., 2014; Yasaka et al., 2010). Additionally, a recent detailed investigation of spinal glycinergic neurons suggests that a small number of islet, central and vertical cells in the SDH are glycinergic (Miranda et al., 2022). In Fig. 3 we report that 3/20 TF neurons (15%) had dendritic characteristics suggesting they are islet cells (RC > 400 μm with a short DV; Table 1). However, as the dendritic patterns of these three neurons were not 'typical' (Light & Kavookjian, 1985; Yasaka et al., 2010), and because of the large range of morphologies we observed for our SDH target neurons, we cannot make any assertions as to which TF neurons might be inhibitory, or which DF neurons might be excitatory. The SDH target neurons we sampled had a variety of firing patterns (DF>TF>PF>>AF>GF) and morphologies (non-classifiable ≈ vertical > radial ≈ central > islet) indicating that they are made up of both inhibitory and excitatory interneurons. Along with previous anatomical work (Aicher et al., 2012; Antal et al., 1996; Miranda et al., 2022), this strongly suggests that the outcome of activation of inhibitory RVM inputs will depend on the function of their SDH target and its position in the spinal nociceptive circuit.

Our observation that all oIPSCs contain a substantial glycinergic component was unexpected, as immunohistochemical and ultrastructural data in fixed tissue indicated that this synapse is largely GABAergic (Aicher et al., 2012; Antal et al., 1996; Light & Kavookjian,

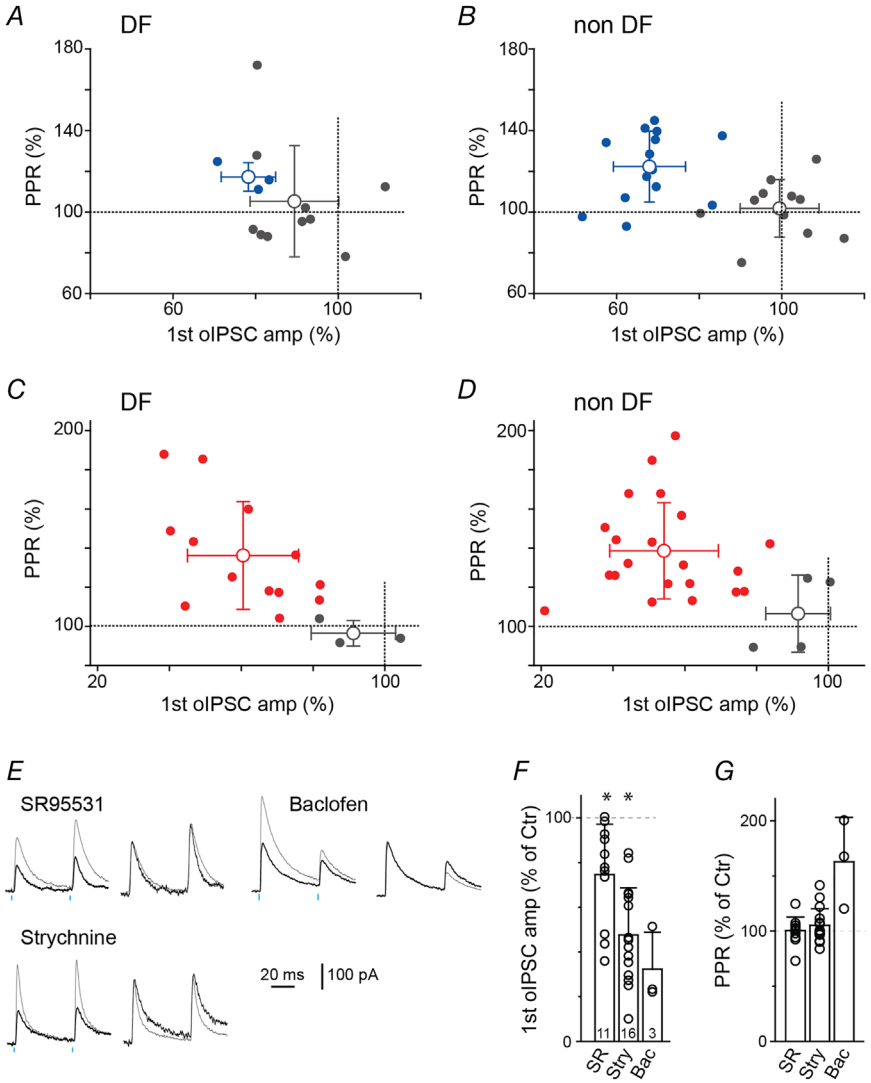

Figure 7. Correlation of opioid effects on amplitude and PPR
Graphs highlighting the relationship between the percentage oIPSC amplitude change in the presence of a μ- (blue; *A* and *B*) or κ- (red; *C*, and *D*) opioid receptor agonists and its relationship to the percentage change in PPR measured from DF (*A* and *C*) or non-DF (*B* and *D*) neurons. Dotted lines at 100% indicates the point where the oIPSC amplitude or PPR was unaltered by the opioid agonist. Coloured and grey dots are neurons where an opioid agonist stimulated inhibition of oIPSC amplitude was detected and not detected, respectively (see Methods). Open circles and bars indicate means ± SD. *E*, pairs of oIPSCs recorded in control solution (grey) or following superfusion with agonists for $GABA_A$, glycine or an antagonist for $GABA_B$-receptors (SR95531, strychnine and 10 μM baclofen, respectively; black). Right: oIPSCs normalised to the peak of the 1st oIPSC. *F* and *G*, quantification of drug effects on the oIPSC peak current (*F*) and PPR (*G*). Individual data points (open circles) and the total number of cells treated with drugs are indicated. Data represent means ± SD. Wilcoxon signed-rank test was used to compare between pre- and post-drug responses. [Colour figure can be viewed at wileyonlinelibrary.com]

© 2022 The Authors. *The Journal of Physiology* published by John Wiley & Sons Ltd on behalf of The Physiological Society.

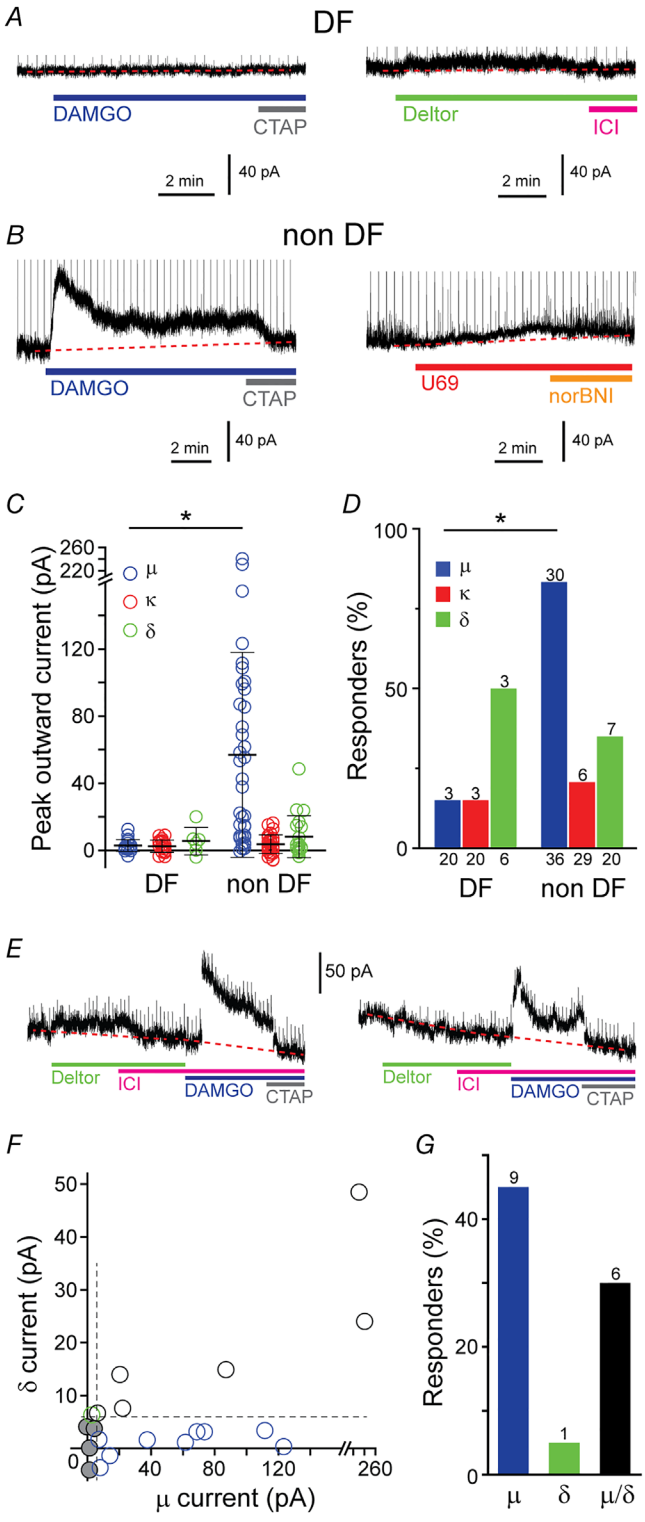

Figure 8. Postsynaptic opioid responses of SDH target neurons
Examples of holding current traces in two DF (*A*) and two non-DF (*B*) neurons during superfusion of the μ-, δ- and κ-opioid agonists (DAMGO, U69593 and deltorphin II, respectively) and when specific antagonists were applied (CTAP, nor BNI and ICI174864 respectively). Dotted lines indicate baseline and vertical lines are truncated oIPSCs. *C*, quantification of peak outward currents induced by opioid agonists from DF and non-DF type neurons. The μ-opioid agonist showed a larger effect in non-DF compared with in DF neurons (Mann-Whitney test). Bars indicate means ± SD. *D*, the proportion of DF and non-DF neurons that have holding current responses to the three opioid receptor agonists. Values on top of the bars indicate the number of responding SDH neurons and those below the bars indicate the total number of cells treated. Fisher's exact test. *E*, example concatenated traces from two SDH target neurons where both DAMGO and deltorphin II (left) and only DAMGO (right) changed holding currents (left). *F*, correlation of the amplitude of the peak outward current measured in response to μ- and δ-agonists in this subset of neurons (n = 20). Cells where the outward current measured were below the responder threshold (dotted lines, 6 pA) are indicated (grey circles). *G*, proportion of neurons shown in *F* that respond to both μ- and δ-opioid receptor agonists (black), or to either μ- alone (blue) or δ-agonists alone (green). The number of responding neurons is indicated on top of each bar. [Colour figure can be viewed at wileyonlinelibrary.com]

1985). As both GABA and glycine modulate neuronal excitability by activating chloride permeable receptors, it could be that these neurotransmitter systems have overlapping functional roles and GABA and glycine corelease serve to secure descending inhibitory transmission (e.g. redundancy) (Hnasko & Edwards, 2012). However, inhibitory signalling is also shaped by a number of other factors including, extrasynaptic $GABA_A$ receptors and metabotropic $GABA_B$ receptors (Chery & De Koninck, 1999; Grudt & Henderson, 1998), $GABA_A$ and glycine receptors' permeability to HCO_3^- altering channel conductance under certain conditions (Kaila & Voipio, 1987; Lückermann et al., 1997; Staley & Proctor, 1999), and glycine co-agonist activity at excitatory *N*-methyl-D-aspartate receptors (Ahmadi et al., 2003). Additionally, because signalling through each receptor is differentially modulated by endogenous and exogenous compounds (Lynch, 2009; Miller & Smart, 2010), it is possible that each inhibitory transmitter has a specialised functional role at this synapse. For example, our finding that RVM inputs onto DF neurons have a glycine-dominant phenotype and are most strongly modulated by presynaptic κ-opioid receptors could result in a shorter inhibitory time course (Anderson et al., 2009; Smith et al., 2016) and a consistent modulation when dynorphin is released, compared to non-DF neurons. Further, a previous study found that excitatory neurons in lamina II–III receive glycine dominant miniature IPSCs and showed that this dominance was altered by peripheral inflammation (Takazawa et al., 2017). Thus, the heterogeneous quality of RVM inhibition at DF compared to non-DF target neurons may not only contribute to the functional role of descending inhibition in spinal nociceptive control but may also play a part in the spinal adaptations that take place in response to prolonged noxious stimuli.

© 2022 The Authors. *The Journal of Physiology* published by John Wiley & Sons Ltd on behalf of The Physiological Society.

Opioid modulation of the RVM to SDH synapse

Despite their many limitations, opioids are still the gold standard for analgesia. Opioid mediated analgesia is facilitated by their actions at opioid receptors expressed at both pre- and postsynaptic sites within the central and peripheral nociceptive systems. The main presynaptic spinal targets of κ-opioid receptor agonists are the central terminals of glutamatergic primary sensory afferents, as no presynaptic κ-effects on IPSCs or EPSCs generated by stimulating neurons/fibres within spinal cord have been reported (Hori et al., 1992; Kohno et al., 1999) (Wu et al., 2003). Our finding that κ-opioid agonists presynaptically disinhibit the descending inhibitory input into the SDH is interesting for a few reasons. Firstly, given the scarcity of presynaptic kappa effects at central synapses in the SDH (Hori et al., 1992; Kohno et al., 1999), detection of a kappa agonists effects on spinal or supraspinal evoked IPSCs in the SDH, especially those accompanied by a PPR change, probably indicates that the recorded neuron receives descending input from the RVM. Secondly, a recent paper investigating the behavioural effects of stimulating KOR$^+$ RVM neurons that project to the cord reported that 80% of these neurons are inhibitory and that their activation is anti-nociceptive in a range of acute and chronic pain behaviours and itch (Nguyen et al., 2022). This study does not examine the spinal connections or pre/postsynaptic expression pattern of κ-opioid expression as we have done here, but its results are consistent with our finding that inhibitory RVM terminals in the cord are reliably inhibited by κ-opioid agonists. We speculate that together these findings suggest that KOR$^+$ RVM neurons are the main RVM neuronal subtype to terminate in the SDH. In addition, electrophysiological recordings of inhibitory RVM descending projection neurons in brainstem slices show the majority of these cells display postsynaptic currents in response to μ-, δ- and κ-opioid receptor agonists (Francois et al., 2017; Kiefel et al., 1993; Marinelli et al., 2002; Pan et al., 1997; Pedersen et al., 2011; Winkler et al., 2006). μ-Opioid-mediated responses are most common and a mix of both μ- and κ-opioid receptor responses are measured in ∼20% of inhibitory RVM projection neurons (Marinelli et al., 2002). Our demonstration that κ-opioid agonists consistently modulate the SDH terminal of RVM projections neurons suggests that opioid receptors may be differentially expressed in the somatic and terminal compartments of RVM-projection neurons. However, as we employed viral vectors to express channelrhodopsins in RVM projection neurons, alterations in circuit organisation, synaptic transmission properties and axonal morphology due to the use of these

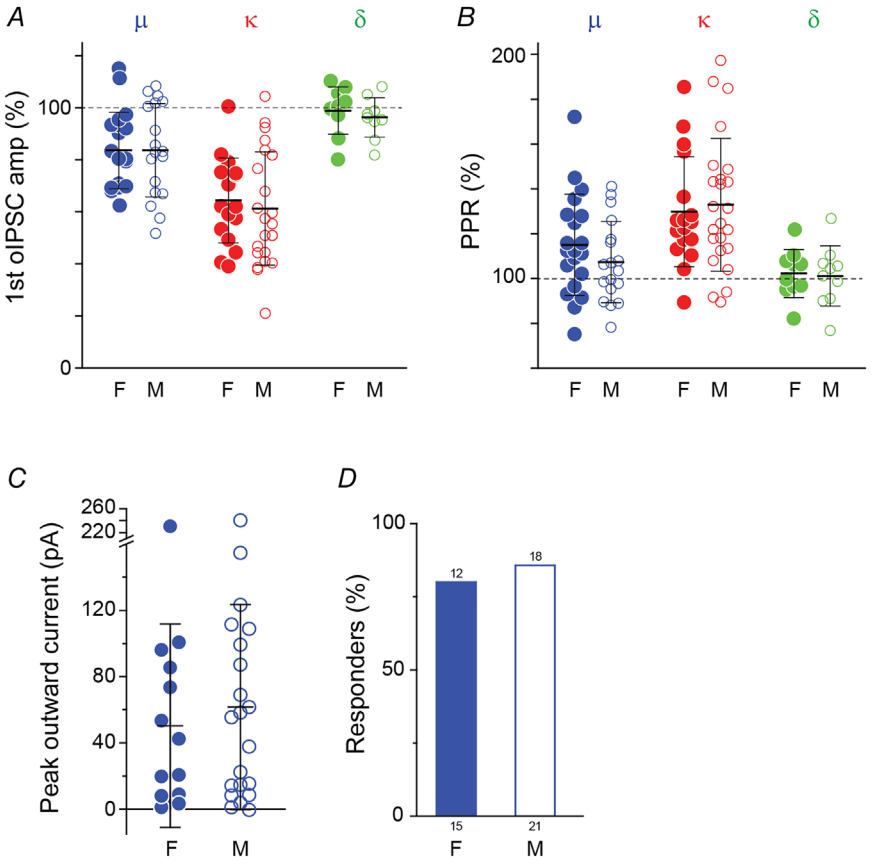

Figure 9. The effects of opioid receptor agonists on oIPSCs recorded from female and male rats were similar
A and *B*, graphs showing the effect of μ-, κ- and δ-opioid agonists (DAMGO, U69593 and deltorphin II respectively) on the oIPSC peak amplitude (*A*) and PPR (*B*) in tissue from female (F, closed circles) and male (M, open circles) rats (μ: 20 cells (F), 18 cells (M); κ: 17 cells (F), 24 cells (M); δ: 10 cells (F), 10 cells (M), two-tailed unpaired *t* test). *C*, changes in holding current of non-DF neurons induced by DAMGO (Mann-Whitney test) and (*D*) the proportion of neurons did not show significant differences between in male and female rats (Fisher's exact test). Values on top of the bars indicate the number of responding non-DF neurons and those below the bars indicate the total number of cells treated. Bars in *A*–*C* indicate means ± SD. [Colour figure can be viewed at wileyonlinelibrary.com]

© 2022 The Authors. *The Journal of Physiology* published by John Wiley & Sons Ltd on behalf of The Physiological Society.

technologies must also be considered (Jackman et al., 2014; Miyashita et al., 2013).

Functional relevance of RVM to SDH signalling and modulation by opioids

RVM inputs to the dorsal horn of the spinal cord have long been known to both facilitate and inhibit spinal nociceptive transmission (Zhou & Gebhart, 1990; Zhuo, 2017), and different cohorts of RVM projection neurons are activated during different behavioural states (Gautier et al., 2017; Gebhart, 2004; Heinricher et al., 2009).

Optogenetic activation and inhibition of the GABAergic RVM input into the dorsal horn of the spinal cord has recently been shown to facilitate and reduce withdrawal behaviours in response to mechanical stimulation, respectively (Francois et al., 2017), suggesting that bidirectional control can be achieved by altering the activity of inhibitory RVM inputs into the spinal cord. Although this finding was interpreted in the context of these inputs making monosynaptic contacts with tonic-firing-enkephalin^{+}-GABAergic interneurons in the spinal cord (Francois et al., 2017), our data highlighting that inhibitory RVM inputs interact with multiple types of SDH interneurons, including TF neurons suggests that the behavioural outcomes of RVM signalling in the SDH is likely to be more complex. Indeed, other studies used *in vivo* electrophysiology to record GABA- and glycine-mediated IPSCs in the SDH of anaesthetised rats (Kato et al., 2006) or chemogenetics to selectively activate KOR-Cre^{+} positive GABAergic RVM neurons in mice suggests that activation of descending inhibitory RVM neurons is analgesic (Kato et al., 2006; Nguyen et al., 2022), can reduce hypersensitivity in chronic pain models and supresses itch (Nguyen et al., 2022). Even though these behavioural outcomes contrast with the findings of Francois et al. (2017), it should be noted that all three studies (and ours) use a non-physiological stimulation to simultaneously activate major parts of the descending RVM input, in some cases for extended periods of time, which could influence the behavioural outcome (see Staley & Proctor, 1999). Thus, the nociceptive roles reported for inhibitory RVM inputs into the cord may reflect different experimental setups interrogating separate parts of a complex circuit that is responsible for integrating multiple sensory modalities to dynamically respond to threat (Francois et al., 2017; Gebhart, 2004). One approach that may lead to a clearer understanding of the role this circuit plays in spinal nociceptive control is to first identify cohorts of RVM projection neurons that fire in response to a particular noxious modality, and then carry out behavioural experiments and selectively activate these neurons using more physiological firing patterns (Dugue et al., 2014; DeNardo & Luo, 2017).

If the majority of RVM inputs to the SDH are part of the neuronal subset identified using the KOR-Cre^{+} mice (Nguyen et al., 2022), it is tempting to predict the outcome of spinal elevations of κ-opioid receptor agonists or the endogenous opioid dynorphin would be pro-nociceptive. This is in line with research indicating that spinal elevations in dynorphin following the development of chronic pain contribute to the descending pathways' maintenance of hyperalgesia (Wang et al., 2001; Burgess et al., 2002; Luo et al., 2008). However, it does not integrate other spinal changes that occur when chronic pain develops. For example, changes in the expression of opioid receptors (Kononenko et al., 2018), non-opioid receptor-mediated dynorphin effects (Podvin et al., 2016), and hypofunction of the potassium-chloride co-transporter KCC2 (Coull et al., 2003; Lee & Prescott, 2015; Lorenzo et al., 2020). Our data showing that inhibitory inputs from the RVM target a wide range of SDH neurons which are differentially modulated by opioids suggests that the behavioural outcomes will depend on the spinal connectivity of the specific RVM cohorts engaged and the dynamic activity of the spinal nociceptive circuit.

References

Abraira, V. E., Kuehn, E. D., Chirila, A. M., Springel, M. W., Toliver, A. A., Zimmerman, A. L., Orefice, L. L., Boyle, K. A., Bai, L., Song, B. J., Bashista, K. A., O'Neill, T. G., Zhuo, J., Tsan, C., Hoynoski, J., Rutlin, M., Kus, L., Niederkofler, V., Watanabe, M., … Ginty, D. D. (2017). The cellular and synaptic architecture of the mechanosensory dorsal horn. *Cell*, **168**(1–2), 295–310.e19.

Ahmadi, S., Muth-Selbach, U., Lauterbach, A., Lipfert, P., Neuhuber, W. L., & Zeilhofer, H. U. (2003). Facilitation of spinal NMDA receptor currents by spillover of synaptically released glycine. *Science*, **300**(5628), 2094–2097.

Aicher, S. A., Hermes, S. M., Whittier, K. L., & Hegarty, D. M. (2012). Descending projections from the rostral ventromedial medulla (RVM) to trigeminal and spinal dorsal horns are morphologically and neurochemically distinct. *Journal of Chemical Neuroanatomy*, **43**(2), 103–111.

Anderson, W. B., Graham, B. A., Beveridge, N. J., Tooney, P. A., Brichta, A. M., & Callister, R. J. (2009). Different forms of glycine- and GABA(A)-receptor mediated inhibitory synaptic transmission in mouse superficial and deep dorsal horn neurons. *Molecular Pain*, **5**, 1744–8069-5–65.

Antal, M., Petko, M., Polgar, E., Heizmann, C. W., & Storm-Mathisen, J. (1996). Direct evidence of an extensive GABAergic innervation of the spinal dorsal horn by fibres descending from the rostral ventromedial medulla. *Neuroscience*, **73**(2), 509–518.

Bailey, P. L., Rhondeau, S., Schafer, P. G., Lu, J. K., Timmins, B. S., Foster, W., Pace, N. L., & Stanley, T. H. (1993). Dose-response pharmacology of intrathecal morphine in human volunteers. *Anesthesiology*, **79**(1), 49–59.

© 2022 The Authors. *The Journal of Physiology* published by John Wiley & Sons Ltd on behalf of The Physiological Society.

Basbaum, A. I., & Fields, H. L. (1984). Endogenous pain control systems: Brainstem spinal pathways and endorphin circuitry. *Annual Review of Neuroscience*, **7**(1), 309–338.

Borgbjerg, F. M., Frigast, C., Madsen, J. B., & Mikkelsen, L. F. (1996). The effect of intrathecal opioid-receptor agonists on visceral noxious stimulation in rabbits. *Gastroenterology*, **110**(1), 139–146.

Browne, T. J., Gradwell, M. A., Iredale, J. A., Maden, J. F., Callister, R. J., Hughes, D. I., Dayas, C. V., & Graham, B. A. (2020). Transgenic cross-referencing of inhibitory and excitatory interneuron populations to dissect neuronal heterogeneity in the dorsal horn. *Frontiers in Molecular Neuroscience*, **13**, 32.

Burgess, S. E., Gardell, L. R., Ossipov, M. H., Malan, T. P., Jr., Vanderah, T. W., Lai, J., & Porreca, F. (2002). Time-dependent descending facilitation from the rostral ventromedial medulla maintains, but does not initiate, neuropathic pain. *The Journal of Neuroscience : The Official Journal of the Society for Neuroscience*, **22**(12), 5129–5136.

Cai, Y. Q., Wang, W., Hou, Y. Y., & Pan, Z. Z. (2014). Optogenetic activation of brainstem serotonergic neurons induces persistent pain sensitization. *Molecular Pain*, **10**, 1744–8069-10-70.

Chery, N., & De Koninck, Y. (1999). Junctional versus extrajunctional glycine and GABAA receptor- mediated IPSCs in identified lamina i neurons of the adult rat spinal cord. *The Journal of neuroscience : The Official Journal of the Society for Neuroscience*, **19**(17), 7342–7355.

Corder, G., Castro, D. C., Bruchas, M. R., & Scherrer, G. (2018). Endogenous and exogenous opioids in pain. *Annual Review of Neuroscience*, **41**(1), 453–473.

Coull, J. A. M., Bourdreau, D., Bachand, K., Prescott, S. A., Nault, F., Sik, A., De Koninck, P., & De Koninck, Y. (2003). Trans-synaptic shift in anion gradient in spinal lamina I neurons as a mechanism of neuropathic pain. *Nature*, **424**(6951), 938–942.

Custodio-Patsey, L., Donahue, R. R., Fu, W., Lambert, J., Smith, B. N., & Taylor, B. K. (2020). Sex differences in kappa opioid receptor inhibition of latent postoperative pain sensitization in dorsal horn. *Neuropharmacology*, **163**, 107726.

Danzebrink, R. M., Green Sa Fau - Gebhart, G. F., & Gebhart, G. F. (1995). Spinal mu and delta, but not kappa, opioid-receptor agonists attenuate responses to noxious colorectal distension in the rat. *Pain*, **63**(1), 39–47.

DeNardo, L., & Luo, L. (2017). Genetic strategies to access activated neurons. *Current Opinion in Neurobiology*, **45**, 121–129.

Dugue, G. P., Lorincz, M. L., Lottem, E., Audero, E., Matias, S., Correia, P. A., Lena, C., & Mainen, Z. F. (2014). Optogenetic recruitment of dorsal raphe serotonergic neurons acutely decreases mechanosensory responsivity in behaving mice. *Plos One*, **9**(8), e105941.

Eckert, W. A., 3rd, & Light, A. R. (2002). Hyperpolarization of substantia gelatinosa neurons evoked by mu-, kappa-, delta 1-, and delta 2-selective opioids. *The Journal of Pain : Official Journal of the American Pain Society*, **3**(2), 115–125.

Fioravante, D., & Regehr, W. G. (2011). Short-term forms of presynaptic plasticity. *Current Opinion in Neurobiology*, **21**(2), 269–274.

Francois, A., Low, S. A., Sypek, E. I., Christensen, A. J., Sotoudeh, C., Beier, K. T., Ramakrishnan, C., Ritola, K. D., Sharif-Naeini, R., Deisseroth, K., Delp, S. L., Malenka, R. C., Luo, L., Hantman, A. W., & Scherrer, G. (2017). A brainstem-spinal cord inhibitory circuit for mechanical pain modulation by GABA and enkephalins. *Neuron*, **93**(4), 822–839.e6.

Gautier, A., Geny, D., Bourgoin, S., Bernard, J. F., & Hamon, M. (2017). Differential innervation of superficial versus deep laminae of the dorsal horn by bulbo-spinal serotonergic pathways in the rat. *IBRO Reports*, **2**, 72-80.

Gebhart, G. F. (2004). Descending modulation of pain. *Neuroscience and Biobehavioral Reviews*, **27**(8), 729–737.

Gerhold, K. J., Drdla-Schutting, R., Honsek, S. D., Forsthuber, L., & Sandkuhler, J. (2015). Pronociceptive and anti-nociceptive effects of buprenorphine in the spinal cord dorsal horn cover a dose range of four orders of magnitude. *The Journal of Neuroscience : the Official Journal of the Society for Neuroscience*, **35**(26), 9580–9594.

Glaum, S. R., Miller, R. J., & Hammond, D. L. (1994). Inhibitory actions of delta 1-, delta 2-, and mu-opioid receptor agonists on excitatory transmission in lamina II neurons of adult rat spinal cord. *The Journal of Neuroscience : the Official Journal of the Society for Neuroscience*, **14**(8), 4965–4971.

Goodchild, C. S., & Gent, J. P. (1992). Spinal cord effects of drugs used in anaesthesia. *General Pharmacology*, **23**(6), 937–944.

Grudt, T. J., & Henderson, G. (1998). Glycine and GABAA receptor-mediated synaptic transmission in rat substantia gelatinosa: Inhibition by mu-opioid and GABAB agonists. *The Journal of Physiology*, **507**(2), 473–483.

Grudt, T. J., & Perl, E. R. (2002). Correlations between neuronal morphology and electrophysiological features in the rodent superficial dorsal horn. *The Journal of Physiology*, **540**(1), 189–207.

Haring, M., Zeisel, A., Hochgerner, H., Rinwa, P., Jakobsson, J. E. T., Lonnerberg, P., La Manno, G., Sharma, N., Borgius, L., Kiehn, O., Lagerstrom, M. C., Linnarsson, S., & Ernfors, P. (2018). Neuronal atlas of the dorsal horn defines its architecture and links sensory input to transcriptional cell types. *Nature Neuroscience*, **21**(6), 869–880.

Heinricher, M. M., Tavares, I., Leith, J. L., & Lumb, B. M. (2009). Descending control of nociception: Specificity, recruitment and plasticity. *Brain Research Reviews*, **60**(1), 214–225.

Hnasko, T. S., & Edwards, R. H. (2012). Neurotransmitter corelease: Mechanism and physiological role. *Annual Review of Physiology*, **74**(1), 225–243.

Hori, Y., Endo, K., & Takahashi, T. (1992). Presynaptic inhibitory action of enkephalin on excitatory transmission in superficial dorsal horn of rat spinal cord. *The Journal of Physiology*, **450**(1), 673–685.

Hossaini, M., Goos, J. A., Kohli, S. K., & Holstege, J. C. (2012). Distribution of glycine/GABA neurons in the ventromedial medulla with descending spinal projections and evidence for an ascending glycine/GABA projection. *Plos One*, **7**(4), e35293.

© 2022 The Authors. *The Journal of Physiology* published by John Wiley & Sons Ltd on behalf of The Physiological Society.

Jackman, S. L., Beneduce, B. M., Drew, I. R., & Regehr, W. G. (2014). Achieving high-frequency optical control of synaptic transmission. *The Journal of Neuroscience : The Official Journal of the Society for Neuroscience*, **34**(22), 7704–7714.

Kaila, K., & Voipio, J. (1987). Postsynaptic fall in intracellular pH induced by GABA-activated bicarbonate conductance. *Nature*, **330**(6144), 163–165.

Kato, G., Yasaka, T., Katafuchi, T., Furue, H., Mizuno, M., Iwamoto, Y., & Yoshimura, M. (2006). Direct GABAergic and glycinergic inhibition of the substantia gelatinosa from the rostral ventromedial medulla revealed by in vivo patch-clamp analysis in rats. *The Journal of Neuroscience : The Official Journal of the Society for Neuroscience*, **26**(6), 1787–1794.

Kerchner, G. A., & Zhuo, M. (2002). Presynaptic suppression of dorsal horn inhibitory transmission by μ-opioid receptors. *Journal of Neurophysiology*, **88**(1), 520–522.

Kiefel, J. M., Rossi, G. C., & Bodnar, R. J. (1993). Medullary mu and delta receptors modulate mesencephalic morphine analgesia in rats. *Brain Research*, **624**(1–2), 151–161.

Kim, H. J., Seol, T. K., Lee, H. J., Yaksh, T. L., & Jun, J. H. (2011). The effect of intrathecal mu, delta, kappa, and alpha-2 agonists on thermal hyperalgesia induced by mild burn on hind paw in rats. *Journal of Anesthesia*, **25**(6), 884–891.

Kim, Y. R., Shim, H. G., Kim, C. E., & Kim, S. J. (2018). The effect of micro-opioid receptor activation on GABAergic neurons in the spinal dorsal horn. *The Korean Journal of Physiology & Pharmacology*, **22**(4), 419–425.

Kohno, T., Kumamoto, E., Higashi, H., Shimoji, K., & Yoshimura, M. (1999). Actions of opioids on excitatory and inhibitory transmission in substantia gelatinosa of adult rat spinal cord. *The Journal of Physiology*, **518**(3), 803–813.

Kohno, T., Moore, K. A., Baba, H., & Woolf, C. J. (2003). Peripheral nerve injury alters excitatory synaptic transmission in lamina II of the rat dorsal horn. *The Journal of Physiology*, **548**(1), 131–138.

Kononenko, O., Mityakina, I., Galatenko, V., Watanabe, H., Bazov, I., Gerashchenko, A., Sarkisyan, D., Iatsyshyna, A., Yakovleva, T., Tonevitsky, A., Marklund, N., Ossipov, M. H., & Bakalkin, G. (2018). Differential effects of left and right neuropathy on opioid gene expression in lumbar spinal cord. *Brain Research*, **1695**, 78–83.

Kumamoto, E., Mizuta, K., & Fujita, T. (2011). Opioid actions in primary-afferent fibers—involvement in analgesia and anesthesia. *Pharmaceuticals*, **4**(2), 343–365.

Labrakakis, C., Rudolph, U., & De Koninck, Y. (2014). The heterogeneity in GABAA receptor-mediated IPSC kinetics reflects heterogeneity of subunit composition among inhibitory and excitatory interneurons in spinal lamina II. *Frontiers in Cellular Neuroscience*, **8**, 424.

Lau, B. K., & Vaughan, C. W. (2014). Descending modulation of pain: The GABA disinhibition hypothesis of analgesia. *Current Opinion in Neurobiology*, **29**, 159–164.

Lau, B. K., Winters, B. L., & Vaughan, C. W. (2020). Opioid presynaptic disinhibition of the midbrain periaqueductal grey descending analgesic pathway. *British Journal of Pharmacology*, **177**(10), 2320–2332.

Lee, K. Y., & Prescott, S. A. (2015). Chloride dysregulation and inhibitory receptor blockade yield equivalent disinhibition of spinal neurons yet are differentially reversed by carbonic anhydrase blockade. *Pain.*, **156**(12), 2431–2437,

Light, A. R., & Kavookjian, A. M. (1985). The ultrastructure and synaptic connections of the spinal terminations from single, physiologically characterized axons descending in the dorsolateral funiculus from the mid-line, pontomedullary region. *The Journal of Comparative Neurology*, **234**(4), 549–560.

Lorenzo, L. E., Godin, A. G., Ferrini, F., Bachand, K., Plasencia-Fernandez, I., Labrecque, S., Girard, A. A., Boudreau, D., Kianicka, I., Gagnon, M., Doyon, N., Ribeiro-da-Silva, A., & De Koninck, Y. (2020). Enhancing neuronal chloride extrusion rescues alpha2/alpha3 GABAA-mediated analgesia in neuropathic pain. *Nature Communications*, **11**(1), 869.

Loyd, D. R., & Murphy, A. Z. (2014). The neuroanatomy of sexual dimorphism in opioid analgesia. *Experimental Neurology*, **259**, 57–63.

Lückermann, M., Trapp, S., & Ballanyi, K. (1997). GABA- and glycine-mediated fall of intracellular pH in rat medullary neurons in situ. *Journal of Neurophysiology*, **77**(4), 1844–1852.

Luo, M. C., Chen, Q., Ossipov, M. H., Rankin, D. R., Porreca, F., & Lai, J. (2008). Spinal dynorphin and bradykinin receptors maintain inflammatory hyperalgesia. *The Journal of Pain : Official Journal of the American Pain Society*, **9**(12), 1096–1105.

Lynch, J. W. (2009). Native glycine receptor subtypes and their physiological roles. *Neuropharmacology*, **56**(1), 303–309.

Marinelli, S., Vaughan, C. W., Schnell, S. A., Wessendorf, M. W., & Christie, M. J. (2002). Rostral ventromedial medulla neurons that project to the spinal cord express multiple opioid receptor phenotypes. *Journal of Neuroscience*, **22**(24), 10847-10855.

Merighi, A. (2018). The histology, physiology, neurochemistry and circuitry of the substantia gelatinosa Rolandi (lamina II) in mammalian spinal cord. *Progress in Neurobiology*, **169**, 91–134.

Millan, M. J. (2002). Descending control of pain. *Progress in Neurobiology*, **66**(6), 355–474.

Miller, P. S., & Smart, T. G. (2010). Binding, activation and modulation of Cys-loop receptors. *Trends in Pharmacological Sciences*, **31**(4), 161–174.

Miranda, C. O., Hegedus, K., Wildner, H., Zeilhofer, H. U., & Antal, M. (2022). Morphological and neurochemical characterization of glycinergic neurons in laminae I-IV of the mouse spinal dorsal horn. *The Journal of Comparative Neurology*, **530**(3), 607–626.

Miyashita, T., Shao, Y. R., Chung, J., Pourzia, O., & Feldman, D. E. (2013). Long-term channelrhodopsin-2 (ChR2) expression can induce abnormal axonal morphology and targeting in cerebral cortex. *Frontiers in Neural Circuits*, **7**, 8.

Mogil, J. S. (2020). Qualitative sex differences in pain processing: emerging evidence of a biased literature. *Nature reviews Neuroscience*, **21**(7), 353–365.

© 2022 The Authors. *The Journal of Physiology* published by John Wiley & Sons Ltd on behalf of The Physiological Society.

Morgan, M. M., Heinricher, M. M., & Fields, H. L. (1992). Circuitry linking opioid-sensitive nociceptive modulatory systems in periaqueductal gray and spinal cord with rostral ventromedial medulla. *Neuroscience*, **47**(4), 863–871.

Nguyen, E., Smith, K. M., Cramer, N., Holland, R. A., Bleimeister, I. H., Flores-Felix, K., Silberberg, H., Keller, A., Le Pichon, C. E., & Ross, S. E. (2022). Medullary kappa-opioid receptor neurons inhibit pain and itch through a descending circuit. *Brain : A Journal of Neurology*, **145**(7), 2586–2601.

Ossipov, M. H., Morimura, K., & Porreca, F. (2014). Descending pain modulation and chronification of pain. *Current Opinion in Supportive and Palliative Care*, **8**(2), 143–151.

Pan, Z. Z., Tershner, S. A., & Fields, H. L. (1997). Cellular mechanism for anti-analgesic action of agonists of the kappa-opioid receptor. *Nature*, **389**(6649), 382–385.

Pedersen, N. P., Vaughan, C. W., & Christie, M. J. (2011). Opioid receptor modulation of GABAergic and serotonergic spinally projecting neurons of the rostral ventromedial medulla in mice. *Journal of Neurophysiology*, **106**(2), 731–740.

Petreanu, L., Mao, T., Sternson, S. M., & Svoboda, K. (2009). The subcellular organization of neocortical excitatory connections. *Nature*, **457**(7233), 1142–1145.

Podvin, S., Yaksh, T., & Hook, V. (2016). The emerging role of spinal dynorphin in chronic pain: A therapeutic perspective. *Annual Review of Pharmacology and Toxicology*, **56**(1), 511–533.

Polgar, E., Wright, L. L., & Todd, A. J. (2010). A quantitative study of brainstem projections from lamina I neurons in the cervical and lumbar enlargement of the rat. *Brain Research*, **1308**, 58–67.

Prescott, S. A., & De Koninck, Y. (2002). Four cell types with distinctive membrane properties and morphologies in lamina I of the spinal dorsal horn of the adult rat. *The Journal of Physiology*, **539**(3), 817–836.

Punnakkal, P., von Schoultz, C., Haenraets, K., Wildner, H., & Zeilhofer, H. U. (2014). Morphological, biophysical and synaptic properties of glutamatergic neurons of the mouse spinal dorsal horn. *The Journal of Physiology*, **592**(4), 759–776.

Randic, M., Cheng, G., & Kojic, L. (1995). kappa-opioid receptor agonists modulate excitatory transmission in substantia gelatinosa neurons of the rat spinal cord. *The Journal of Neuroscience : The Official Journal of the Society for Neuroscience*, **15**(10), 6809–6826.

Ruscheweyh, R., Ikeda, H., Heinke, B., & Sandkuhler, J. (2004). Distinctive membrane and discharge properties of rat spinal lamina I projection neurones in vitro. *The Journal of Physiology*, **555**(2), 527–543.

Santos, S. F. A., Melnick, I. V., & Safronov, B. V. (2004). Selective postsynaptic inhibition of tonic-firing neurons in substantia gelatinosa by μ-opioid agonist. *Anesthesiology*, **101**(5), 1177–1183.

Schmauss, C. (1987). Spinal kappa-opioid receptor-mediated antinociception is stimulus-specific. *European Journal of Pharmacology*, **137**(2–3), 197–205.

Smith, K. M., Boyle, K. A., Madden, J. F., Dickinson, S. A., Jobling, P., Callister, R. J., Hughes, D. I., & Graham, B. A. (2015). Functional heterogeneity of calretinin-expressing neurons in the mouse superficial dorsal horn: implications for spinal pain processing. *The Journal of Physiology*, **593**(19), 4319–4339.

Smith, K. M., Boyle, K. A., Mustapa, M., Jobling, P., Callister, R. J., Hughes, D. I., & Graham, B. A. (2016). Distinct forms of synaptic inhibition and neuromodulation regulate calretinin-positive neuron excitability in the spinal cord dorsal horn. *Neuroscience*, **326**, 10–21.

Snyder, L. M., Chiang, M. C., Loeza-Alcocer, E., Omori, Y., Hachisuka, J., Sheahan, T. D., Gale, J. R., Adelman, P. C., Sypek, E. I., Fulton, S. A., Friedman, R. L., Wright, M. C., Duque, M. G., Lee, Y. S., Hu, Z., Huang, H., Cai, X., Meerschaert, K. A., Nagarajan, V., … Ross S. E. (2018). Kappa opioid receptor distribution and function in primary afferents. *Neuron*, **99**(6), 1274–1288.e6.

Staley, K. J., & Proctor, W. R. (1999). Modulation of mammalian dendritic GABA(A) receptor function by the kinetics of Cl- and HCO3- transport. *The Journal of Physiology*, **519**(3), 693–712.

Takazawa, T., Choudhury, P., Tong, C. K., Conway, C. M., Scherrer, G., Flood, P. D., Mukai, J., & MacDermott, A. B. (2017). Inhibition mediated by glycinergic and GABAergic receptors on excitatory neurons in mouse superficial dorsal horn is location-specific but modified by inflammation. *The Journal of Neuroscience : The Official Journal of the Society for Neuroscience*, **37**(9), 2336–2348.

Todd, A. J. (2010). Neuronal circuitry for pain processing in the dorsal horn. *Nature Reviews Neuroscience*, **11**(12), 823–836.

Todd, A. J. (2017). Identifying functional populations among the interneurons in laminae I-III of the spinal dorsal horn. *Molecular Pain*, **13**, 174480691769300.

Wang, D., Tawfik, V. L., Corder, G., Low, S. A., Francois, A., Basbaum, A. I., & Scherrer, G. (2018). Functional divergence of delta and mu opioid receptor organization in CNS pain circuits. *Neuron*, **98**(1), 90-108.e5.

Wang, Z., Gardell, L. R., Ossipov, M. H., Vanderah, T. W., Brennan, M. B., Hochgeschwender, U., Hruby, V. J., Malan, T. P., Jr., Lai, J., & Porreca, F. (2001). Pronociceptive actions of dynorphin maintain chronic neuropathic pain. *The Journal of Neuroscience : The Official Journal of the Society for Neuroscience*, **21**(5), 1779–1786.

WeiWei, Y., WenDi, F., Mengru, C., Tuo, Y., & Chen, G. (2021). The cellular mechanism by which the rostral ventromedial medulla acts on the spinal cord during chronic pain. *Reviews in the Neurosciences*, **32**(5), 545–558.

Winkler, C. W., Hermes, S. M., Chavkin, C. I., Drake, C. T., Morrison, S. F., & Aicher, S. A. (2006). Kappa opioid receptor (KOR) and GAD67 immunoreactivity are found in OFF and NEUTRAL cells in the rostral ventromedial medulla. *Journal of Neurophysiology*, **96**(6), 3465–3473.

Winters, B. L., Gregoriou, G. C., Kissiwaa, S. A., Wells, O. A., Medagoda, D. I., Hermes, S. M., Burford, N. T., Alt, A., Aicher, S. A., & Bagley, E. E. (2017). Endogenous opioids regulate moment-to-moment neuronal communication and excitability. *Nature Communications*, **8**(1), 14611.

© 2022 The Authors. *The Journal of Physiology* published by John Wiley & Sons Ltd on behalf of The Physiological Society.

Wu, S. Y., Ohtubo, Y., Brailoiu, G. C., & Dun, N. J. (2003). Effects of endomorphin on substantia gelatinosa neurons in rat spinal cord slices. *British Journal of Pharmacology*, **140**(6), 1088–1096.

Yaksh, T. L. (1987). Spinal opiates: A review of their effect on spinal function with emphasis on pain processing. *Acta Anaesthesiologica Scandinavica Supplementum*, **31**, 25–37.

Yang, K., Ma, W. L., Feng, Y. P., Dong, Y. X., & Li, Y. Q. (2002). Origins of GABA(B) receptor-like immunoreactive terminals in the rat spinal dorsal horn. *Brain Research Bulletin*, **58**(5), 499–507.

Yasaka, T., Tiong, S. Y., Hughes, D. I., Riddell, J. S., & Todd, A. J. (2010). Populations of inhibitory and excitatory interneurons in lamina II of the adult rat spinal dorsal horn revealed by a combined electrophysiological and anatomical approach. *Pain*, **151**(2), 475–488.

Yu, W., Pati, D., Pina, M. M., Schmidt, K. T., Boyt, K. M., Hunker, A. C., Zweifel, L. S., McElligott, Z. A., & Kash, T. L. (2021). Periaqueductal gray/dorsal raphe dopamine neurons contribute to sex differences in pain-related behaviors. *Neuron*, **109**(8), 1365–1380.e5.

Zhang, Y., Zhao, S., Rodriguez, E., Takatoh, J., Han, B. X., Zhou, X., & Wang, F. (2015). Identifying local and descending inputs for primary sensory neurons. *The Journal of Clinical Investigation*, **125**(10), 3782–3794.

Zhou, M., & Gebhart, G. F. (1990). Characterization of descending inhibition and facilitation from the nuclei reticularis gigantocellularis and gigantocellularis pars alpha in the rat. *Pain*, **42**(3), 337–350.

Zhuo, M. (2017). Descending facilitation. *Molecular Pain*, **13**, 174480691769921.

Zhuo, M., & Gebhart, G. F. (1990). Characterization of descending inhibition and facilitation from the nuclei reticularis gigantocellularis and gigantocellularis pars alpha in the rat. *Pain (Amsterdam)*, **42**, 337–350.

Zorman, G., Belcher, G., Adams, J. E., & Fields, H. L. (1982). Lumbar intrathecal naloxone blocks analgesia produced by microstimulation of the ventromedial medulla in the rat. *Brain Research*, **236**(1), 77–84.

Additional information

Data availability statement

Data is available on request from the corresponding authors.

Competing interests

The authors have no conflict of interest to disclose.

Author contributions

All experiments were carried out at the Kolling Institute. Y.O. and K.A. designed and carried out experiments, analysed and interpreted data and wrote the manuscript. Both authors have approved the final version of the manuscript and agree to be accountable for all aspects of the work. All persons designated as authors qualify for authorship, and all those who qualify for authorship are listed.

Funding

This work was supported by the Pain Foundation (ABN 87072480123) and the Ernest Heine Family Foundation (ABN 29405919488). K.A. and Y.O. are employees of NSW Health.

Acknowledgements

Thanks to Chris Vaughan and Bryony Winters for critical comments and Sherelle Casey, Eddy Sokolaj and Claudia Natal for technical assistance. The viral vectors used in this study to express channelrhodopsins were kind gifts from Edward Boyden or Karl Deisseroth.

Open access publishing facilitated by The University of Sydney, as part of the Wiley – The University of Sydney agreement via the Council of Australian University Librarians.

Keywords

descending pain pathway, inhibitory neurotransmission, IPSC, optogenetics, raphe-spinal tract, substantia gelatinosa

Supporting information

Additional supporting information can be found online in the Supporting Information section at the end of the HTML view of the article. Supporting information files available:

Statistical Summary Document
Peer Review History

© 2022 The Authors. *The Journal of Physiology* published by John Wiley & Sons Ltd on behalf of The Physiological Society.